

Chip Formation Analysis and Machining Optimization of Titanium Ti6Al4V



Author

MUHAMMAD UZAIR SAJJAD

Regn # 00000328869

Supervisor

DR SYED HUSSAIN IMRAN

DEPARTMENT OF MECHANICAL ENGINEERING
SCHOOL OF MECHANICAL & MANUFACTURING ENGINEERING
NATIONAL UNIVERSITY OF SCIENCES AND TECHNOLOGY
ISLAMABAD
MAY 2024

Chip Formation Analysis and Machining Optimization of Titanium
Ti6Al4V

Author

MUHAMMAD UZAIR SAJJAD

Regn # 00000328869

A thesis submitted in partial fulfillment of the requirements for the degree of
MS Mechanical Engineering

Thesis Supervisor:

DR SYED HUSSAIN IMRAN

DEPARTMENT OF MECHANICAL ENGINEERING
SCHOOL OF MECHANICAL & MANUFACTURING ENGINEERING
NATIONAL UNIVERSITY OF SCIENCES AND TECHNOLOGY,
ISLAMABAD
MAY 2024

National University of Sciences and Technology

MASTER THESIS WORK

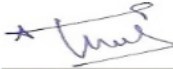
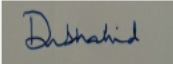


Form TH-4


National University of Sciences & Technology (NUST)
MASTER'S THESIS WORK

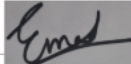
We hereby recommend that the dissertation prepared under our supervision by: Muhammad uzair Sajjad (00000328869) Titled: Chip Formation Analysis and Machining Optimization of Titanium Ti6Al4V be accepted in partial fulfillment of the requirements for the award of MS in Mechanical Engineering degree.

Examination Committee Members

- | | | |
|----|-------------------------------|--|
| 1. | Name: Aamir Mubashar | Signature:  |
| 2. | Name: Shahid Ikram Ullah Butt | Signature:  |

Supervisor: Syed Hussain Imran Jaffery

Signature: 
Date: 19 - Apr - 2024

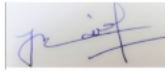


Head of Department

19 - Apr - 2024

Date

COUNTERSIGNED



Dean/Principal

19 - Apr - 2024

Date

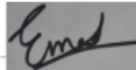
THESIS ACCEPTANCE CERTIFICATE

Certified that final copy of MS/MPhil thesis written by Regn No. 00000328869 Muhammad uzair Sajjad of School of Mechanical & Manufacturing Engineering (SMME) has been vetted by undersigned, found complete in all respects as per NUST Statues/Regulations, is free of plagiarism, errors, and mistakes and is accepted as partial fulfillment for award of MS/MPhil degree. It is further certified that necessary amendments as pointed out by GEC members of the scholar have also been incorporated in the said thesis titled. **Chip Formation Analysis and Machining Optimization of Titanium Ti6Al4V**

Signature: 

Name (Supervisor): Syed Hussain Imran Jaffery

Date: 19 - Apr - 2024

Signature (HOD): 

Date: 19 - Apr - 2024

Signature (DEAN): 

Date: 19 - Apr - 2024

Plagiarism Certificate (Turnitin Report)

This thesis has been checked for Plagiarism. Turnitin report endorsed by Supervisor is attached.



MUHAMMAD UZAIR SAJJAD

REGN # 00000328869



DR SYED HUSSAIN IMRAN

(SUPERVISOR)

Declaration

I certify that this research work titled “*Chip Formation Analysis and Machining Optimization of Titanium Ti6Al4V*” is my own work. The work has not been presented elsewhere for assessment. The material that has been used from other sources it has been properly acknowledged / referred.



MUHAMMAD UZAIR SAJJAD

REGN # 00000328869

Copyright Statement

- Copyright in text of this thesis rests with the student author. Copies (by any process) either in full, or of extracts, may be made only in accordance with instructions given by the author and lodged in the Library of NUST School of Mechanical & Manufacturing Engineering (SMME). Details may be obtained by the Librarian. This page must form part of any such copies made. Further copies (by any process) may not be made without the permission (in writing) of the author.
- The ownership of any intellectual property rights which may be described in this thesis is vested in NUST School of Mechanical & Manufacturing Engineering, subject to any prior agreement to the contrary, and may not be made available for use by third parties without the written permission of the SMME, which will prescribe the terms and conditions of any such agreement.
- Further information on the conditions under which disclosures and exploitation may take place is available from the Library of NUST School of Mechanical & Manufacturing Engineering, Islamabad.

Acknowledgements

I am thankful to my Creator (ﻯ ﺗﻌﺎﻝ ﺳﺒﺨﺎﻧﻪ ﺑﻠﻻ) who has guided me throughout this work at every step and for every new thought which You set up in my mind to improve it. Indeed, I could have done nothing without Your priceless help and guidance. Whosoever helped me throughout the course of my thesis, whether my parents or any other individual was Your will, so indeed none be worthy of praise but You.

Dedicated to my parents and supervisor whose tremendous support and cooperation led me to this wonderful accomplishment.

Abstract

The advancement in the materials science domain has led to the development of many robust composite alloys yielding high tensile strength, low density, and good corrosion resistance. One of such materials is the Titanium-Aluminum-Vanadium Alloy Ti6Al4V. The addition of Aluminum and Vanadium compounds enhances the overall material hardness in the alloy matrix, thus improving its physical and mechanical properties. During Orthogonal cutting, the flow stress distribution, cutting forces, and surface finish of the working material play a vital role in predicting the material response via utilizing the Finite Element Analysis (FEA) methodology coupled with the Arbitrary Eulerian-Lagrangian (ALE) meshing during simulations performed in ABAQUS platform in orthogonal cutting analysis. The Johnson-Cook (J-C) model is utilized in finite element analysis of metal cutting as it can efficiently model considerations for temperature-dependent visco-plasticity, higher material strain rates, and larger von mises stresses, while incorporating key features including strain hardening of material, strain rate sensitivity, and heat softening. Our Research aims to formulate a Numerical Finite Element Analysis (FEA) based Model which incorporates a wider range of Johnson-Cook (JC) model test sets totaling to 32 simulated sets of JC Parameters (A, B, C, m, and n) in order to identify the optimum JC test set which would allow us to confirm the model characteristics including Cutting Force, Chip Morphology and Surface Finish, Feed Force/Reaction Force, and Von Mises Stress Distribution during the orthogonal cutting of the Ti6Al4V material. Furthermore, the analysis will provide insights into optimizing machining parameters to enhance productivity, minimize tool wear, and improve surface quality in Ti6Al4V machining operations.

Key Words: *Orthogonal Cutting, Chip Morphology, Johnston Cook Parameters, Titanium Aluminum Vanadium, Finite Element Analysis*

Table of Contents

Thesis Acceptance Certificate	iii
Plagiarism Certificate (Turnitin Report)	v
Declaration	vi
Copyright Statement	vii
Acknowledgements	viii
Abstract	x
Table of Contents	xi
List of Figures	xiii
List of Tables	xiv
1. CHAPTER 1: INTRODUCTION	1
1.1. Background.....	1
1.1.1. Work piece and Tool.....	1
1.1.2. Orthogonal Cutting	2
1.1.3. Plasticity and Johnson Cook Model.....	2
1.1.4. Stress and Strain in specimens under discussion	3
1.2. Problems and Objectives of the Research.....	3
1.3. Scope of the Thesis	4
1.4. Thesis Outline.....	4
2. CHAPTER 2: Literature Review	6
2.1. Metal Cutting Processes	6
2.1.1. Orthogonal Cutting	6
2.1.2. Oblique Cutting	8
2.2. Analytical Cutting Models.....	9
2.2.1. Johnson Cutting (JC) Model	9
2.2.2. Coupled Eulerian-Lagrangian (CEL) Model	9
2.2.3. Arbitrary Lagrangian-Eulerian (ALE) Model.....	10
2.3. Chip Morphology	10
2.3.1. Discontinuous Chips (Type I).....	11
2.3.2. Continuous Chips without Built Up Edge (BUE) (Type II).....	12
2.3.3. Continuous Chips with Built Up Edge (BUE) (Type III)	12
2.3.4. Serrated/Segmented Chips (Type IV)	12
2.4. Tool Wear and Workpiece Machined Surface Topography	13
2.5. Coated and Uncoated Tools.....	14
2.6. Temperature Profile.....	14
2.7. Cooling Approaches	15
2.7.1. Dry Cutting	15

2.7.2.	Cryogenic Cutting.....	16
2.7.3.	Emulsion Cutting	16
2.8.	Cutting and Feed Forces	17
2.9.	Cutting Speed	18
2.10.	Microstructure Evolution.....	19
2.11.	Deformation Modelling	20
2.12.	FEM Optimization.....	21
3.	CHAPTER 3: Finite Element Modelling	22
3.1.	Work piece and Tool Material and Geometry	22
3.2.	Cutting Parameters Identification	24
3.3.	Cutting Model Selection (JC Model).....	24
3.4.	Meshing and Adaptive Meshing	25
3.5.	Boundary Conditions	26
3.6.	FEM Software Selection.....	27
4.	CHAPTER 4: Johnson Cook Parameters for Simulation Modelling.....	28
4.1.	Selection of JC Parameters	28
4.2.	Evaluation of JC Parameters.....	28
5.	CHAPTER 5: Orthogonal Cutting Experimentation and Simulation	30
5.1.	Experimental Set Up.....	31
5.1.1.	Cutting and Feed Forces	32
5.1.2.	Chip Morphology.....	33
5.2.	Simulation Set Up.....	34
5.2.1.	Finite Element Model	35
5.2.2.	Work piece Mechanical Model.....	35
5.2.3.	Tool Mechanical Model.....	36
5.2.4.	Cutting Forces Evaluation	36
5.2.5.	Chip Formation Analysis.....	37
5.3.	Comparison between Experiment and Simulation.....	37
5.3.1.	Cutting and Feed Forces	38
5.3.2.	Chip Formation.....	39
5.4.	Discussion	40
5.4.1.	Impact of Chip Morphology on Material Surface Finish and Tool Life	41
5.4.2.	Impact of Cutting Forces on Material Surface Finish and Tool Life	42
5.4.3.	Impact of Mesh Density on Accuracy of Model.....	43
6.	CHAPTER 6: Conclusions and Future Recommendations	44
6.1.	Conclusions	44
6.2.	Future Recommendations	44
APPENDIX	46

List of Figures

Figure 1. Effective strain rate contours trend obtained for orthogonal cutting model (Tyan & Yang, 1992).....	7
Figure 2. Stress distribution diagrams generally obtained for oblique cutting model (Lin & Lin, 1999).....	8
Figure 3. Initiation of discontinuous chip and the corresponding von Mises stress contour (Guo & Yen, 2004)	11
Figure 4. Propagation of discontinuous chips and the corresponding von Mises stress contour (Guo & Yen, 2004)	11
Figure 5. Schematic of segmented chip (Kountanya, Zkeri, & Altan, 2009).....	13
Figure 6. Variation of wear with machining time (Ambadekar & Choudhari, 2020)	14
Figure 7. Comparison of experimental and numerically evaluated cutting forces (top) and tangential forces (bottom) for both dry and cryogenic cutting under different operating conditions (Rotella, 2014)	16
Figure 8. Comparison of cutting force and thrust force against the cutting speed for different feed rates f for the titanium alloy Ti_6Al_4V (Fang & Wu, 2009).....	17
Figure 9. Schematic diagram of variations in microstructures occurring in Ti_6Al_4V alloy (Pederson, 2002)	19
Figure 10. Variation of residual stress developed in material with respect to depth of cut (Cheng & Outeiro, 2022).....	20
Figure 11. Geometry of the workpiece (top) and the machining tool (bottom)	23
Figure 12. Mesh configuration for the machining tool (left) and the workpiece (right)	25
Figure 13. Boundary Constraints of Workpiece & Tool piece.	26
Figure 14. Von Mises Stress Contours Distribution during Orthogonal Machining of Tungsten Carbide Workpiece	34
Figure 15. RMS vs Cutting Force for Each Set	39
Figure 16. RMS Feed Force for Each Set	39
Figure 17. Graphical Analysis outlining Von Mises Stress produced during Ti_6Al_4V machining vs Machining Time.....	41

List of Tables

TABLE I: The JC Parameters Outlined for Cumulative Test Sets 1-32 respectively	30
TABLE II: Summarized Cutting Conditions Applied during Ti6Al4V machining process	31
TABLE III: Cutting Parameters Outlined in Tabulated form for JC Test sets 1-32:.....	32

1. CHAPTER 1: INTRODUCTION

The Research Investigates Orthogonal Cutting of a Ti6Al4V Titanium Alloy modelled using the Finite Element Analysis (FEA) based Numerical Modelling technique, incorporating Johnson-Cook (JC) Model Parameters to estimate the overall Cutting force, Feed (Reaction) force, Chip Morphology, Von mises stress distribution, and surface finish parameters during the machining process. The Workpiece and Tool used during the machining process was modelled in 2D workspace using ABAQUS where 32 different JC sets were investigated and enhanced in terms of initial yield strength, flow stress, strain rate effect, thermal softening effect depicting quasi-static strain rate behavior. The model developed was optimized and validated with an experimental investigation by (Ducobu, Rivi`ere-Lorph`evre, & Filippi).

1.1. Background

The Machining Process in particular orthogonal cutting can be regarded as a complicated process involving removal of chips via cutting tool which generates huge amounts of strain and associated stress withing the workpiece. The machined material also is subjected to high thermal stresses which further intensifies the process complexity. Numerical Modelling in particular the Finite Element Analysis (FEA) approach is adopted to simplify the overall phenomena taking place during orthogonal machining of a newer class of material metal-composites – Ti₆Al₄V coupled with the Arbitrary Eulerian-Lagrangian (ALE) formulations modelled using the Johnson-Cook (JC) constitutive model and its parameters.

1.1.1. Work piece and Tool

Ti₆Al₄V, a prevalent titanium alloy belonging to the $\alpha + \beta$ group, represents over half of titanium alloy production (Arrazola, et al., 2009). Ti₆Al₄V is favored as a workpiece for machining due to its exceptional mechanical properties. Firstly, its high strength-to-weight ratio makes it ideal for applications requiring lightweight yet durable components, such as aerospace and medical implants. Additionally, Ti₆Al₄V exhibits excellent corrosion resistance, ensuring longevity and reliability in harsh environments. Furthermore, its good formability allows for intricate machining without sacrificing structural integrity. Secondly, it's combination of α and β phases enables tailored mechanical properties, including high tensile strength, fatigue resistance,

and fracture toughness, making it a versatile choice for a wide range of machining applications.

Tungsten carbide tools are commonly used in the machining of titanium alloys due to their high hardness, wear resistance, and resistance to heat and abrasion. Furthermore, the resistance of tungsten carbide to heat and abrasion is particularly important in the machining of titanium alloys, as these materials tend to generate high temperatures and abrasive wear on cutting tools (Sisodiya & Bajpai, 2013). Tungsten carbide's elevated melting point, combined with its effective heat dissipation capability, enables it to endure the high temperatures generated during machining without experiencing notable deformation or softening (Aleksandra, 2023).

1.1.2. Orthogonal Cutting

Orthogonal cutting provides simplicity in analysis of the machining operation by providing a leeway to the evaluation and accurate measurements of stress contours in three dimensions, while also providing the option of approximation where possible. This would allow for a base case to build up on (Usui, Shirakashi, & Kitagawa, 1978).

In practical orthogonal cutting, the workpiece material undergoes plastic deformation due to interaction with the cutting tool and chip. The material in the chip's interior experiences plane strain deformation and flows perpendicular to the cutting edge, while material near the edges undergoes plane stress deformation and flows along the cutting edge. To ensure orthogonal machining, the chip width-to-thickness ratio must exceed a critical value, ensuring that over 90% of the chip width experiences plane strain deformation (Pednecker, Madhavan, & Adibi-Sedeh, 2004).

1.1.3. Plasticity and Johnson Cook Model

Plasticity and elasticity are distinct material responses to external forces. Elasticity describes a material's ability to deform reversibly under stress, returning to its original shape once the stress is removed. In contrast, plasticity involves permanent deformation beyond the material's elastic limit, leading to a change in shape that is retained even after the stress is removed. While elasticity is characterized by linear stress-strain behavior, plasticity is nonlinear and typically involves the rearrangement of atomic or molecular structures. Plasticity results in permanent changes, making it crucial in processes like metal forming, whereas elasticity ensures materials recover their initial shape, vital for various engineering applications.

The analysis of mechanical parameters is conducted using several models, including the Johnson-Cook (JC) model, the Modified Coulomb-Mohr model, and the Norton-Hoff model. The Johnson-Cook model is a widely employed constitutive model since it offers a comprehensive representation of material response to high strain rates and elevated temperatures. Its incorporation of strain hardening, thermal softening, and strain rate sensitivity allows accurate prediction of material behavior during machining, facilitating optimization of cutting parameters and tool design. Additionally, the JC model's simplicity and compatibility with finite element analysis make it a preferred choice for simulating complex machining processes in diverse industrial applications.

1.1.4. Stress and Strain in specimens under discussion

In machining Ti6Al4V alloy, understanding stress and strain is crucial for optimizing cutting parameters, minimizing tool wear, and ensuring component integrity. Ti6Al4V's unique properties, including its high strength-to-weight ratio and excellent corrosion resistance, make it desirable for aerospace, medical, and automotive applications. However, its complex microstructure and tendency to work harden pose challenges during machining, necessitating accurate stress and strain analysis.

The Johnson-Cook (JC) model offers a valuable tool for this analysis. By incorporating parameters such as strain rate sensitivity and thermal softening, the JC model enables accurate prediction of material behavior under high strain rates and elevated temperatures encountered during machining. This allows engineers to optimize cutting conditions to minimize tool wear and prevent catastrophic failure while achieving desired component properties. Thus, focusing on stress and strain analysis, aided by the JC model, ensures efficient and reliable machining of Ti6Al4V alloy for various industrial applications.

1.2. Problems and Objectives of the Research

The most widely incorporated flow stress model in metal cutting modelling is the Johnson-Cook constitutive model comprising of a wider range of parameters. It often becomes complicated to select the JC test set which would provide the optimum results. Hence, for specified materials, different parameters including strain, strain rates, stress, stress rates and temperature ranges etc. are available pertaining to varying identification conditions.

Our Research Aims to Formulate a Numerical Finite Element Analysis (FEA) based Model which incorporates a wider range of Johnson-Cook (JC) model test sets totaling to 32 simulated sets of JC Parameters (A, B, C, m, and n) in order to identify the optimum JC test set which would allow us to confirm the following model characteristics during the orthogonal cutting of the Ti₆Al₄V material:

- A. Cutting Force
- B. Feed Force/Reaction Force
- C. Chip Morphology and Surface Finish
- D. Von Mises Stress Distribution

Finally, an optimum test once obtained which conforms to the accurate estimation of cutting force, average feed force, and chip thickness values, are used to validate the comparison made to the already published experimental results indicated by (Ducobu, Rivi`ere-Lorph`evre, & Filippi).

1.3. Scope of the Thesis

This project aims to analyze the machining of Ti₆Al₄V alloy using a tungsten carbide tool and simulate the results using Johnson-Cook (JC) parameters. The study will investigate the influence of cutting parameters such as cutting speed, feed rate, and depth of cut on machining forces, tool wear, and surface integrity. Finite Element Method (FEM) simulations incorporating the JC model will be conducted to predict material behavior under various machining conditions. The project will provide insights into optimizing machining parameters to enhance productivity, minimize tool wear, and improve surface quality in Ti₆Al₄V machining operations.

1.4. Thesis Outline

The report discusses the motivation for the domain of research conducted within, followed by brief outline of the conduct and governing concepts. The literature review discusses the general trend of the investigations conducted in the field, which include both the recent studies and those pertaining to the prior, along with graphic references. This review also identifies the limitations of the previous studies, and suggestions on how to improve upon them are given in the later sections.

The methodology discusses the extensive simulation models and optimization models studied during the analysis of machining of titanium alloy Ti₆Al₄V, followed by the procedure of

analysis and the results obtained from the study. These results are then compared with the data from the available literature, and a validation case is then provided to affirm the authenticity of the obtained results along with the procedure followed. The key points from the study are then extracted to form the concluding statement along with any future recommendations were deemed necessary.

2. CHAPTER 2: Literature Review

There is various research available in literature which have investigated the orthogonal machining methodology of Titanium alloys based on the Finite Element Analysis approach, utilizing Johnson Cook constitutive modelling for the estimation of average cutting and feed forces, chip formation and buildup, and von mises stress distribution. Ti₆Al₄V has been largely used and investigated during experimental and numerical analysis by various researchers particularly due to its ability in forming segmented chips during lower cutting speeds, which is unique phenomenon exhibited by other materials at quite higher cutting speed ranges (Komanduri & von Turkovich). In a research by a series of continuous and interrupted orthogonal cutting tests on a specially adapted lathe machining facility were performed where high speed imaging was carried out using microscopic lens and strobed copper-vapor laser illumination at a cycle rate of 24,000 frames/s. The cutting speeds ranged within 4 to 140 m/min. The chip segment geometry, segmentation frequency, critical strain required to initiate shear band formation, were examined outlining the increase in chip segmentation with cutting speed while at the same time, results give added support to the thermoplastic shear instability theory for shear band formation during orthogonal machining of Ti₆Al₄V.

2.1. Metal Cutting Processes

Metal cutting constitutes a multifaceted procedure. Grasping the deformation and alterations in quality occurring on the machined surface of the workpiece material during the cutting process proves instrumental in effectively managing the process's quality and enhancing cutting standards. Consequently, research endeavors in this domain have persisted since the onset of this century.

2.1.1. Orthogonal Cutting

The orthogonal cutting assumes direct motion along the workpiece at a right angle. While the technique is commonly used in metal removal processes to produce a high-quality surface finish, issues such as tool failure and workpiece quality degradation enforce the constant need for optimizing the process. Study of the cutting process revealed that a gradient of stress contours is formed at the contact point where the tool meets the workpiece, and that if the effective strain on

the workpiece is sufficiently drastic, its procedure can lead to a material failure and deterioration of the material quality (Tyan & Yang, 1992).

One of the main causes for the damage to the tool and workpiece is identified to be the influence of friction on the material properties during machining (Shet & Deng, 2000). According to the available literature, the thermomechanical work can lead to a temperature rise of up to 1000°C (Boothroyd, 1961). This necessitates that the stress, strain, and the corresponding contours be studied while considering the temperature gradient of the tool as well as the workpiece during operation in order to be able to provide reasonable control parameters for process optimization.

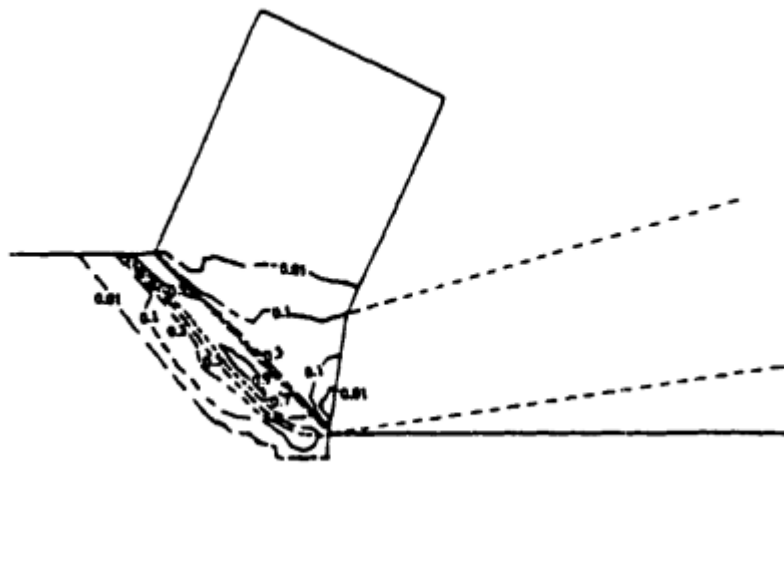


Figure 1. Effective strain rate contours trend obtained for orthogonal cutting model (Tyan & Yang, 1992)

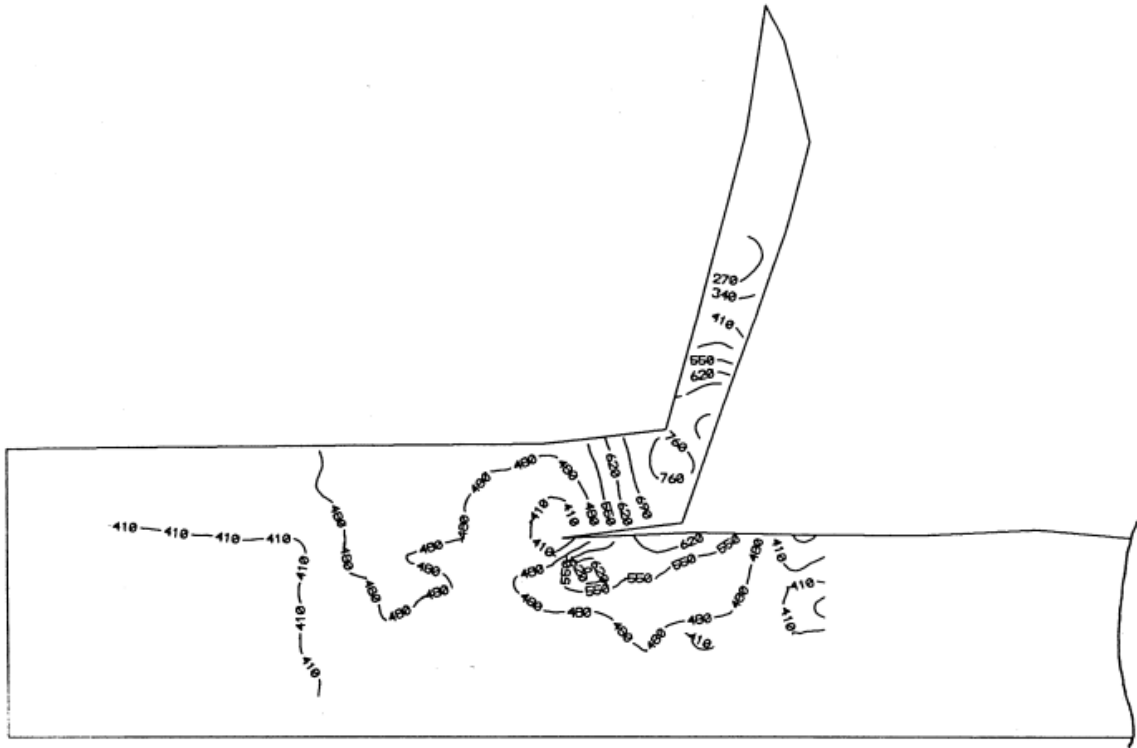


Figure 2. Stress distribution diagrams generally obtained for oblique cutting model (Lin & Lin, 1999)

2.1.2. Oblique Cutting

Contrary to its former counterpart, this procedure maintains a certain angle between the tool and workpiece upon contact. While oblique cutting also faces the operational issues as discussed in the previous section, the stress analysis of the procedure shows that even though the stress propagation initiates from the point of contact, the stress distribution is relatively more spread out (Lin & Lin, 1999).

Another main difference observed when comparing the two procedures is that the cutting force, while remaining generally constant for orthogonal cutting, shows a rapid increase from a smaller magnitude, followed by a gradual constant trend. This can be attributed to the fact that when the tool contacts the workpiece in oblique cutting, the first contact with the workpiece is not the entire edge of the cutting tool, but rather a small portion of it, which gradually increases as the tool cuts through the material.

2.2. Analytical Cutting Models

The analytical models provide a convenient link between machining applications and the underlying theory. The need of cutting models arise in order to simulate the conditions of procedure and identifying the corresponding issues faced. Doing so can allow one to devise an appropriate strategy to tackle the issues such as vibrations of the cutting tool and the regenerative effect of the workpiece (Altintas, 2000). The commonly used empirical models are based on the chip formation and depth of cut as the main governing parameters (Rott, Homberg, & C, 2006). The theoretical models are an amalgamation of the classical physics that is applied to different frames of references based on the feasibility in applications. A more detailed account of the theoretical models is as provided in the below sections.

2.2.1. Johnson Cutting (JC) Model

This model is a classical analytical approach which aims to describe the mechanics of metal cutting. It does so by emphasizing on the interaction between the cutting tool and the workpiece, by considering parameters such as tool geometry, material properties and cutting conditions. The Johnson-Cook model employs simplified assumptions to formulate a mathematical representation which can be used to predict the cutting forces, chip formation, and surface quality of the operation.

The parameters required for modelling the cutting operation can be obtained using regression analysis on pre-existing experimental data (Dorogoy & Rittel, 2009). Similarly, optimization approaches for Johnson cutting parameters for titanium alloys were studied by Lin et al. using a genetic algorithm multi-objective approach (Lin & Yang, 1999). Chen et al. had also derived a Johnson-Cook model for Ti₆Al₄V and made a comparison of simulation outcomes regarding cutting forces and the morphology of machining chips with experimental data (Chen, Ren, Yu, Yang, & Zhang, 2012).

2.2.2. Coupled Eulerian-Lagrangian (CEL) Model

The Coupled Eulerian-Lagrangian (CEL) model is an alternative to the Johnson-Cook model, which employs a finite element method (FEM) to simulate the cutting process, taking into account the material properties, tool geometry, and cutting conditions.

In the CEL model, the cutting tool is modeled as a Lagrangian body, while the workpiece is enclosed by a grid of structural mesh that allows for chip formation and growth. This approach

significantly reduces the complexity of building a FE model for metal cutting compared to the ALE model, which requires a special designed mesh and initial chip geometry (Ducobu F. , et al., 2017).

The CEL model has been successfully employed to model 3D metal cutting processes, and it has been shown to reproduce experimental results and predict trends induced by variations in cutting conditions. The proposed model shows a good ability to reproduce the experimental results and to predict the trends induced by variations in the cutting conditions (Ducobu, et al., 2019).

2.2.3. Arbitrary Lagrangian-Eulerian (ALE) Model

The ALE model operates on the similar analogy to CEL in that it integrates the Lagrangian and Eulerian frameworks in the cutting model, but it offers additional flexibility in handling motion of the material. This is done by discretization of the grid domain so that the mesh can deform and move with the material. This allows for adaptive grid refinement and efficient simulation of large deformations.

The early development of the ALE finite element methods can be found in the works of (Donea, Stella, & Giuliani, 1977) and Liu (Liu, 1981). While the initial models were developed based on the hypo-elastic relations (Benson, 1989) the recent models have considered the deformation gradients in the elastic and plastic regions (Armero & Love, ALE finite element methods for finite strain plasticity and fluid problems, 2001).

Classical ALE formulations account for both the deformation of the reference mesh into the spatial mesh and the velocity of this mesh relative to the material particles. Finite element implementations typically involve nodal displacements and nodal relative velocities of the spatial mesh. The displacements are solved through the physical problem, while the relative velocities are defined through a rezoning algorithm (Armero & Love, 2003).

2.3. Chip Morphology

Titanium alloys pose machining challenges, particularly at high speeds, due to inherent properties. Varying cutting speeds result in distinct chip morphologies, primarily due to changes in crack behavior and flow localization. Chip segmentation induces vibrations, limiting material removal rates and productivity. Understanding chip segmentation's mechanics is crucial for enhancing machinability and tool life in titanium alloy machining, necessitating a focus on its

impact on thermo-mechanical behavior and productivity (Hua & Shivpuri, 2004).

2.3.1. Discontinuous Chips (Type I)

Discontinuous chips are usually formed in hard machining at large speeds for achieving high production efficiency. These chips form during metal cutting when the material undergoes brittle fracture. They consist of separate, discrete segments and are typically associated with materials that exhibit poor ductility or high hardness.

Most of the previous simulations for discontinuous chips were based on the strain-based fracture criterion (Obikawa, Sasahara, Shirakashi, & Usui, 1997). The initiation and propagation of chip cracks are typically simulated by integrating the Johnson-Cook plasticity and damage models (Movahhedy, Gadala, & Altintas, 2000). However, majority of these simulations are proprietary or rely on specific subroutines, restricting accessibility for broader use. The study performed by Guo is aimed to tackle this issue (Guo & Yen, 2004).

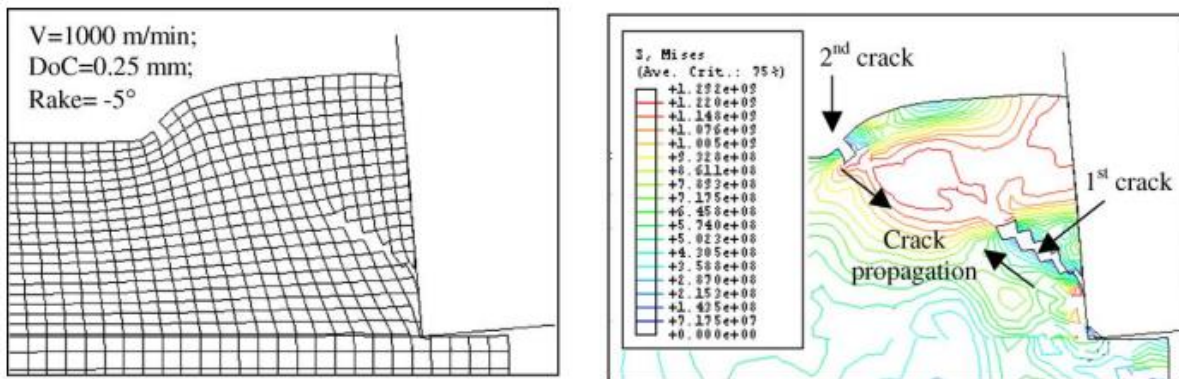


Figure 3. Initiation of discontinuous chip and the corresponding von Mises stress contour (Guo & Yen, 2004)

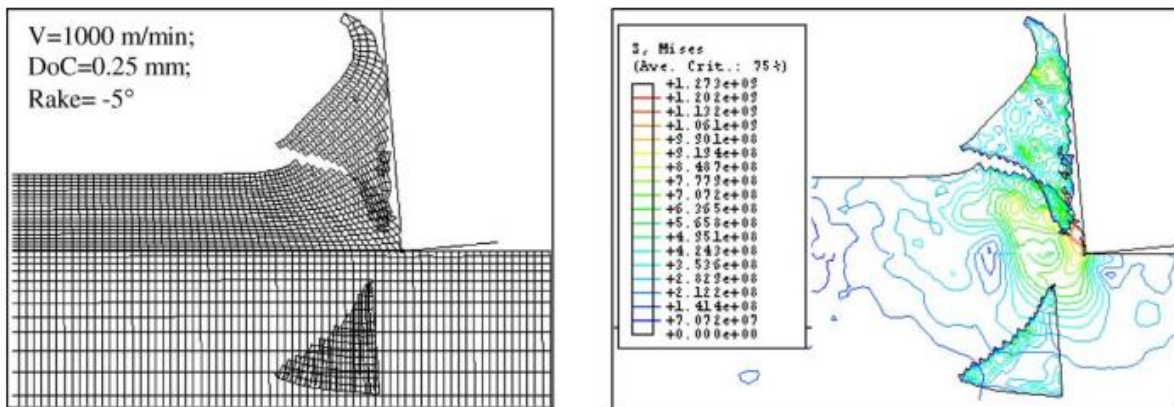


Figure 4. Propagation of discontinuous chips and the corresponding von Mises stress contour (Guo & Yen, 2004)

2.3.2. Continuous Chips without Built Up Edge (BUE) (Type II)

Continuous chips without built-up edge are characteristic of stable metal cutting processes, where material removal occurs smoothly without significant accumulation on the tool edge. Typically observed in materials with good machinability, these chips reflect efficient chip evacuation and minimal frictional interaction between the tool and workpiece. Their formation signifies optimal cutting conditions, leading to enhanced surface finish and prolonged tool life in machining operations.

According to the available literature, the reason for formation of continuous chips without built-up edge is that the chip ratio never exceeds 100% (Kountanya, Zkeri, & Altan, 2009). This value represents the ratio between the average cut chip thickness and the uncut chip thickness, both of which are the average values taken over the sample range. This value of the ratio has been attributed to the fact that the shear angle never exceeds 45° (Connolly & Rubenstein, 1968).

2.3.3. Continuous Chips with Built Up Edge (BUE) (Type III)

Continuous chips with built-up edge occur when material accumulates on the tool edge during cutting, leading to poor surface finish and accelerated tool wear. This phenomenon is particularly problematic in materials prone to adhesion or work hardening. The accumulation of material on the tool edge alters cutting dynamics, increasing frictional forces and promoting wear, ultimately affecting machining quality and tool longevity.

The adhesion of chips to the cutting tool can lead to the formation of a built-up edge (BUE), resulting in increased tool wear rates and potential surface defects such as galling and smearing. Sun et al. observed BUE formation during dry machining of Ti₆Al₄V alloy, with larger BUE sizes at the tool nose corner compared to the tool rake (Sun, Brandt, & John, 2013). Bermingham et al. attributed adhesive interactions to diffusion processes between the tool and adhering material (Bermingham, Palanisamy, & Dargush, 2012).

2.3.4. Serrated/Segmented Chips (Type IV)

Serrated or segmented chips are characterized by their irregular, saw-toothed morphology resulting from intermittent chip flow disruptions. These interruptions occur due to unstable cutting conditions, including vibration or insufficient chip evacuation, which have been demonstrated by the shear-crack hypothesis (SCH) (Shaw & Vyas, 1998). As the cutting tool encounters varying

material properties or geometric irregularities, chip formation becomes erratic, leading to surface quality degradation and potential tool damage. The irregular chip morphology exacerbates machining instabilities, increasing cutting forces and heat generation. Mitigating these issues often involves optimizing cutting parameters, enhancing chip evacuation systems, and employing vibration damping techniques to ensure smoother chip formation and improve overall machining performance.

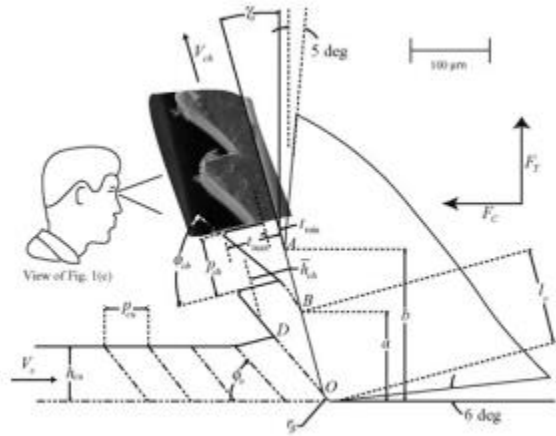


Figure 5. Schematic of segmented chip (Kountanya, Zkeri, & Altan, 2009)

2.4. Tool Wear and Workpiece Machined Surface Topography

As titanium alloys find broader applications, high-speed machining offers benefits like improved surface finish and enhanced material removal rates. Yet, in machining Ti_6Al_4V , high-speed operations accelerate tool wear, elevating manufacturing costs and compromising surface integrity. Addressing severe tool wear and surface quality degradation in Ti_6Al_4V machining is imperative. Balancing the advantages of high-speed machining with the need for prolonged tool life and superior surface finish is essential for efficient titanium alloy manufacturing (Liang & Liu, 2018).

The most prominent mechanisms proposed for tool wear and crater formations are adhesion, dissolution, and diffusion (Venugopal, Paul, & Chattopadhyay, 2007). Tool wear is intensified by the depression of the cutting edge caused by both micro and macro fractures. This phenomenon occurs when fractures at various scales weaken the cutting edge, leading to its deformation. As a result, the tool becomes less effective in material removal and is more prone to further damage, ultimately reducing its lifespan and compromising machining performance.

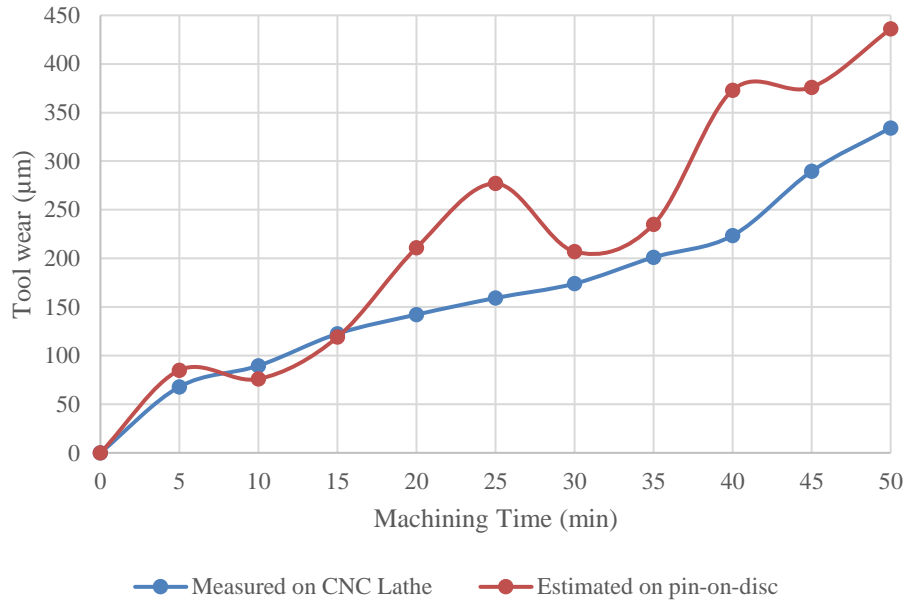


Figure 6. Variation of wear with machining time (Ambadekar & Choudhari, 2020)

2.5. Coated and Uncoated Tools

In the machining of Ti_6Al_4V alloy, both coated and uncoated tools play vital roles in the material removal process. Coated tools, typically with coatings like titanium nitride or titanium aluminum nitride, offer improved wear resistance and reduced friction, enhancing tool life and surface finish. However, their strong affinity with titanium alloys can result in severe adhesive and diffusive wear (Liang & Liu, 2018). Uncoated tools, while generally more economical, may experience higher wear rates but can still provide effective material removal.

Multi-layer coating of titanium alloys on the tools used in the machining of Ti_6Al_4V led to a comparatively harder substrate tool, while enhancing the tool strength (Revuru, Pasam, & Posinasetti, 2020). Coated tools have a better resistance to micro-chipping, which lead to a longer tool life, while preventing formations of tool craters and reducing contact length (Grzesik, 1999).

2.6. Temperature Profile

The dynamics of vibration, stress, and temperature within the machining zone significantly contribute to tool damage (Zhao, Barber, & Zou, 2002). These factors are crucial determinants of machining performance, as they directly influence productivity, tool wear, and surface integrity. Factors such as cutting velocities, depths, coolant application, feed rates, and tool materials play

pivotal roles in shaping these machining conditions (Childs, 2000). Achieving optimal machining outcomes hinges upon carefully balancing these inputs to mitigate tool damage and ensure desirable surface quality.

Despite the advantageous properties of titanium alloys for practical applications, machining them poses exceptional challenges (Bolzoni, Ruiz-Navas, & Gordo, 2017). Titanium alloys exhibit high strength, corrosion resistance, and low thermal conductivity, making them ideal for aerospace and medical applications. However, their unique properties contribute to their difficulty in machining, necessitating careful consideration of machining parameters and tool selection to overcome challenges and achieve desired outcomes.

2.7. Cooling Approaches

Effective cooling approaches are essential in titanium alloy machining to dissipate heat generated during the process. Without proper cooling, elevated temperatures can lead to thermal softening of the workpiece material and accelerated tool wear (Hong, Markus, & Jeong, 2001). Additionally, excessive heat can cause metallurgical changes, such as phase transformations and residual stresses, compromising component integrity and surface finish. Implementing cooling techniques, such as flood coolant or high-pressure coolant systems, helps maintain stable machining conditions, prolong tool life, improve surface quality, and prevent detrimental effects on workpiece properties in titanium alloy machining operations.

2.7.1. Dry Cutting

Dry cutting approach offers simplicity and cost savings by negating the use of coolant fluids during machining operations. However, it poses challenges in titanium alloy machining due to the material's high heat generation and poor thermal conductivity. Without cooling, heat accumulates at the cutting interface, accelerating tool wear, and compromising surface finish (Auchet, Chevrier, Lacour, & Lipinski, 2004). While dry cutting reduces environmental impact and avoids coolant-related issues, its feasibility in titanium alloy machining requires careful consideration of cutting parameters and tool coatings to mitigate thermal effects and ensure satisfactory machining outcomes.

2.7.2. Cryogenic Cutting

Cryogenic cutting involves using liquid nitrogen or other cryogenic fluids to cool the cutting zone, significantly improving the machinability of titanium alloys (Dillon, De Angelis, Lu, Gunasekara, & Deno, 1990). This approach enhances tool life and surface integrity by minimizing heat-affected zones and work hardening in titanium alloy machining. Contrary to the previous approaches, where the cryogenic coolant was flooded on both the workpiece and the machining tool, a more economically viable approach suggests the use of a nozzle between the chip breaker and tool insert to form a fluid-gas cushion to absorb the heat generated due to friction (Hong, Markus, & Jeong, 2001). The process also focuses on cooling the tool instead of the workpiece, since cooling the tool strengthens the material and thus increases the tool life (Zhao & Hong, 1992). Unlike steel, the hardness of Ti₆Al₄V rises rapidly at lower temperatures, which increases the tendency of abrasive wear of the chip to the cutting tool (Ding & Hong, 1998).

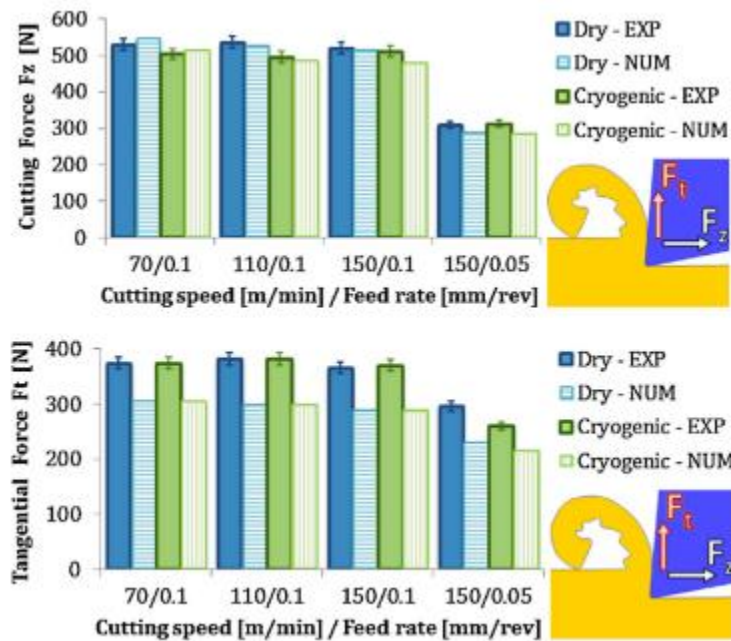


Figure 7. Comparison of experimental and numerically evaluated cutting forces (top) and tangential forces (bottom) for both dry and cryogenic cutting under different operating conditions (Rotella, 2014)

2.7.3. Emulsion Cutting

Emulsion cutting employs water-based cutting fluids mixed with oil or other additives to cool and lubricate the cutting zone in titanium alloy machining. This method offers effective heat

dissipation and chip evacuation, enhancing tool life and surface finish. Emulsions also provide corrosion protection and can improve machining efficiency by reducing friction and preventing built-up edge formation. However, emulsion cutting may pose challenges in managing fluid disposal and environmental impact. Despite these considerations, it remains a widely used and versatile coolant option for titanium alloy machining, offering a balance between performance, cost-effectiveness, and environmental responsibility. Review of available literature shows that emulsion cutting reduces the maximum operating temperature by more than 35% (Hong, Markus, & Jeong, 2001).

2.8. Cutting and Feed Forces

Cutting force is the axial force exerted on the cutting tool during machining processes, influenced by factors such as tool geometry, material properties, and cutting parameters. Accurate prediction of cutting parameters, including forces, chip morphology, temperature fields, and surface integrity, hinges on the precise selection of machining parameters. This step is widely recognized as crucial for ensuring the desired machining outcomes with high accuracy. By

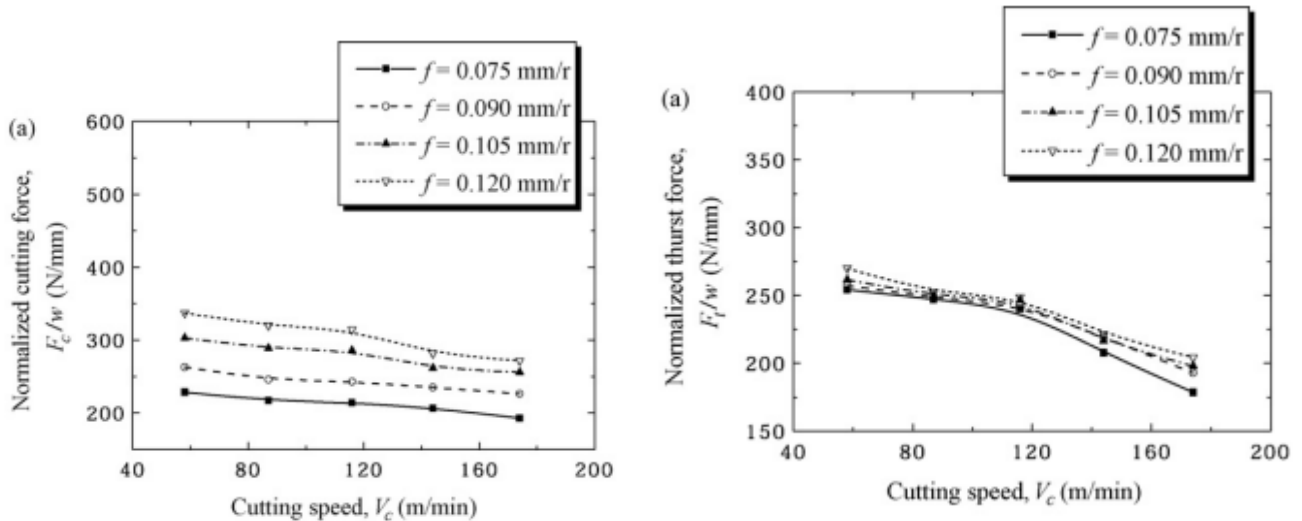


Figure 8. Comparison of cutting force and thrust force against the cutting speed for different feed rates f for the titanium alloy Ti_6Al_4V (Fang & Wu, 2009)

carefully choosing parameters, manufacturers can optimize cutting processes to achieve improved surface quality, dimensional accuracy, and overall productivity in machining operations (Umbrello, 2008). Finite element analysis is favored over extensive experimental work due to its time and cost efficiency. Previous research indicates that its results closely align with experimental findings (Sasahara, Obikawa, & Shirakashi, 2004).

Feed force, also known as tangential force, is the lateral force applied to the cutting tool perpendicular to its motion. It determines the rate at which material is removed along the workpiece surface and affects chip formation and tool wear. Balancing feed force with cutting parameters is essential for achieving optimal material removal rates, surface finish, and dimensional accuracy in machining operations. The work of Kandrac et al. suggests that the feed force increases with the cutting speed and the feed rate. Other parameters considered include the rake angle and cutting-edge radius, which allow for a comprehensive study of the parameters governing the feed cutting force (Kandrac, Mankova, Vrabel, & Beno, 2014).

2.9. Cutting Speed

Cutting speed refers to the relative velocity between the cutting tool and the workpiece material during machining. It directly influences material removal rates, tool wear, and surface finish. Higher cutting speeds generally result in increased productivity but can also lead to elevated temperatures, which may affect tool life and workpiece integrity. Optimal cutting speed selection is critical, balancing the need for efficient material removal with considerations for tool life, surface quality, and machining stability. Adjusting cutting speed based on material properties, tool characteristics, and machining requirements is essential for achieving desired machining outcomes in various industrial applications.

While the variation of cutting speed has no substantial effect on the tangential and feed cutting forces, it shows a strong correlation with the axial cutting force (Krishnaraj, Samsudeensadham, & Kuppan, 2014). Cutting speed can also be related to the operating temperature, in that the temperatures increase with cutting speed, reach a maximum value, followed by a decrement in value at even higher speeds (Schulz, 2004).

2.10. Microstructure Evolution

Despite significant progress in cutting tool material development, equivalent advancements for cutting titanium alloys have been lacking due to their complex microstructure (Nouari & Makich, Experimental investigation on the effect of the material microstructure on tool wear when machining hard titanium alloys: Ti-6Al-4V and Ti-555, 2013). The high-level properties of titanium alloys, influenced by grain size, solid solution atoms, and precipitation hardening, are

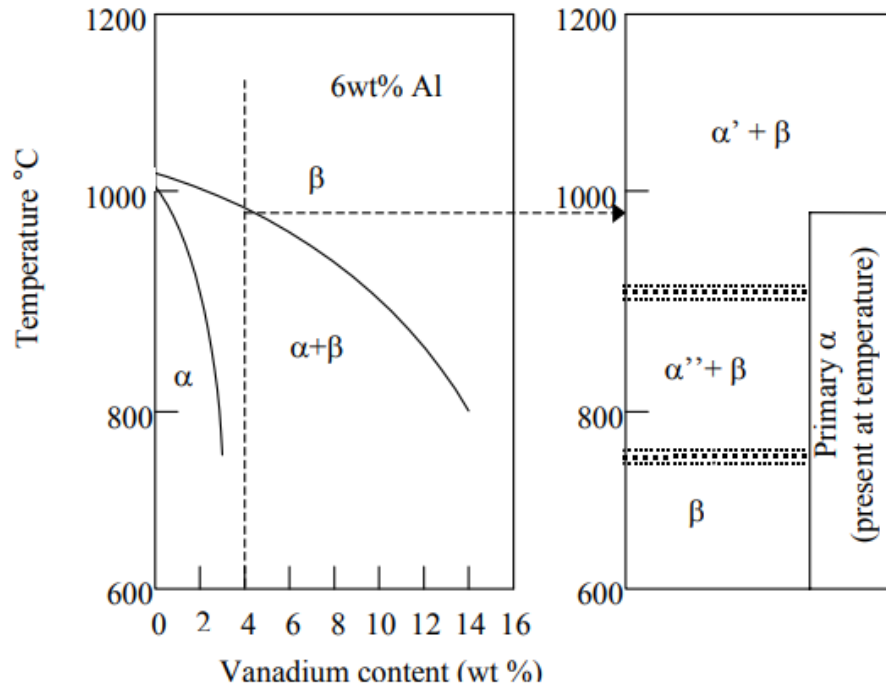


Figure 9. Schematic diagram of variations in microstructures occurring in Ti_6Al_4V alloy (Pederson, 2002)

intricately tied to their specific microstructures, shaped by various forming processes (Clement, Lenain, & Jacques, 2007).

Modifying the microstructure and mechanical characteristics of metal involves a combination of working processes and heat treatments. The addition of elements to titanium, known as alloying, further impacts its microstructure and properties. Depending on the desired phase dominance (α , β , or $\alpha + \beta$), specific alloying elements are introduced to pure titanium to achieve the desired alloy composition and properties (Nouari & Ginting, Wear characteristics and performance of multi-layer CVD-coated alloyed carbide tool in dry end milling of titanium alloy, 2006).

2.11. Deformation Modelling

Deformation modeling for titanium alloys is crucial for understanding and predicting their behavior under various mechanical processes. Titanium alloys are known for their complex microstructures, which include α , β , and $\alpha + \beta$ phases, influencing their mechanical response. Deformation models typically consider factors such as crystallographic texture, grain size, and the presence of alloying elements to accurately simulate the material's behavior. Common modeling approaches include crystal plasticity models, finite element simulations, and continuum mechanics formulations. These models aid in predicting phenomena such as plastic deformation, strain

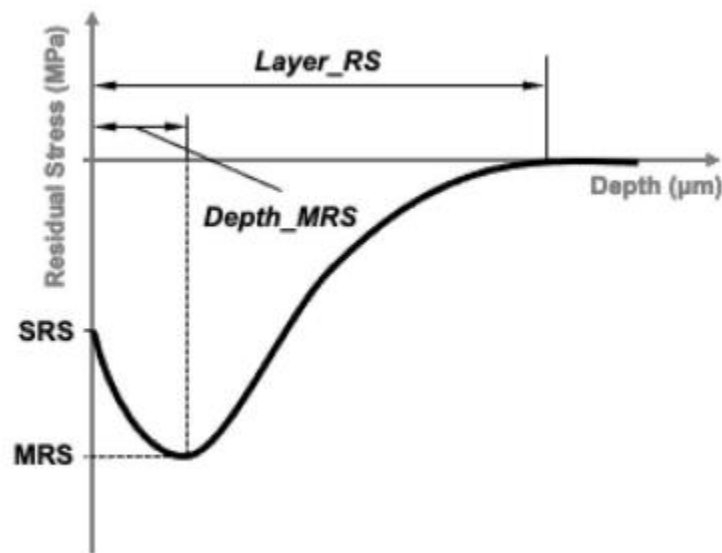


Figure 10. Variation of residual stress developed in material with respect to depth of cut (Cheng & Outeiro, 2022)

hardening, and the development of microstructural features, facilitating the optimization of processing parameters and the design of titanium alloy components for diverse applications.

The material deformation is primarily modelled using the Norton-Hoff constitutive equation; however, it fails to examine the variations in the elasticity of the material (Lopez, 2018). The transition of the titanium alloys from the α to β and vice versa has been attributed to the changed in the temperature, which include both the temperatures during the machining operation as well as prior. Pre-operative annealing also influences the micro-structure of the alloy, and thus has an impact on the phases and grain size present in the material during operation (Li, et al., 2019).

2.12. FEM Optimization

Finite Element Method (FEM) optimization is a powerful tool extensively utilized in the machining of Ti_6Al_4V , a challenging titanium alloy. FEM optimization involves creating computational models to simulate machining processes and iteratively adjusting parameters to achieve desired outcomes. In Ti_6Al_4V machining, FEM optimization enables engineers to optimize cutting parameters such as cutting speed, feed rate, and depth of cut to minimize tool wear, reduce machining forces, and enhance surface integrity. By simulating the complex interactions between the cutting tool, workpiece, and cutting environment, FEM optimization helps identify optimal machining conditions, leading to improved efficiency, productivity, and component quality in Ti_6Al_4V machining applications.

The work of Barile et al. utilized a the FEM in tandem with the Phase-Shifting Electronic Speckle Pattern Interferometry (PS-EPSI) in order to provide an innovative approach to determining the mechanical properties of titanium under machining conditions (Barile, Casavola, Pappalettera, & Pappalettera, *Advanced Approaches for Mechanical Characterization On Innovative Materials*). The FEM model assumes that material as isotropic, which negates the significance of Poisson ratio in the machining model, and instead only relies on the modulus of elasticity for analysis (Barile, Casavola, Pappalettera, & Pappalettera, *Experimental and numerical characterization of sinterized materials with speckle interferometry and optimization methods*, 2011).

3. CHAPTER 3: Finite Element Modelling

The FEM model for the machining of Ti₆Al₄V was formulated using ABAQUS for ease in formulation of the workpiece and tool geometry in the software, along with the convenience of boundary conditions and evaluation of the required results.

3.1. Work piece and Tool Material and Geometry

The machining tool and the workpiece to be considered in the study have been formulated using ABAQUS. The dimensions for both the workpiece as well as the tool are as provided in the figures below. Since the analysis is restricted to two dimensional deformations, the workpiece considered is a rectangular body of dimensions 1mm×0.5mm, while the working tool is given an arbitrary shape based on general profiles available in the literature. The tool tip is ensured to be rounded, since a vertex is virtually impossible in real applications. It should also be considered that the vertex would create a high stress concentration region at the tool tip, and thus the tool itself would deform instead of the workpiece, which would defeat the purpose of the study.

Once the desired geometry for the two components is designed, they are assigned their respective materials. The tool is assigned the properties corresponding to tungsten carbide, while the workpiece is assigned as the titanium alloy Ti₆Al₄V.

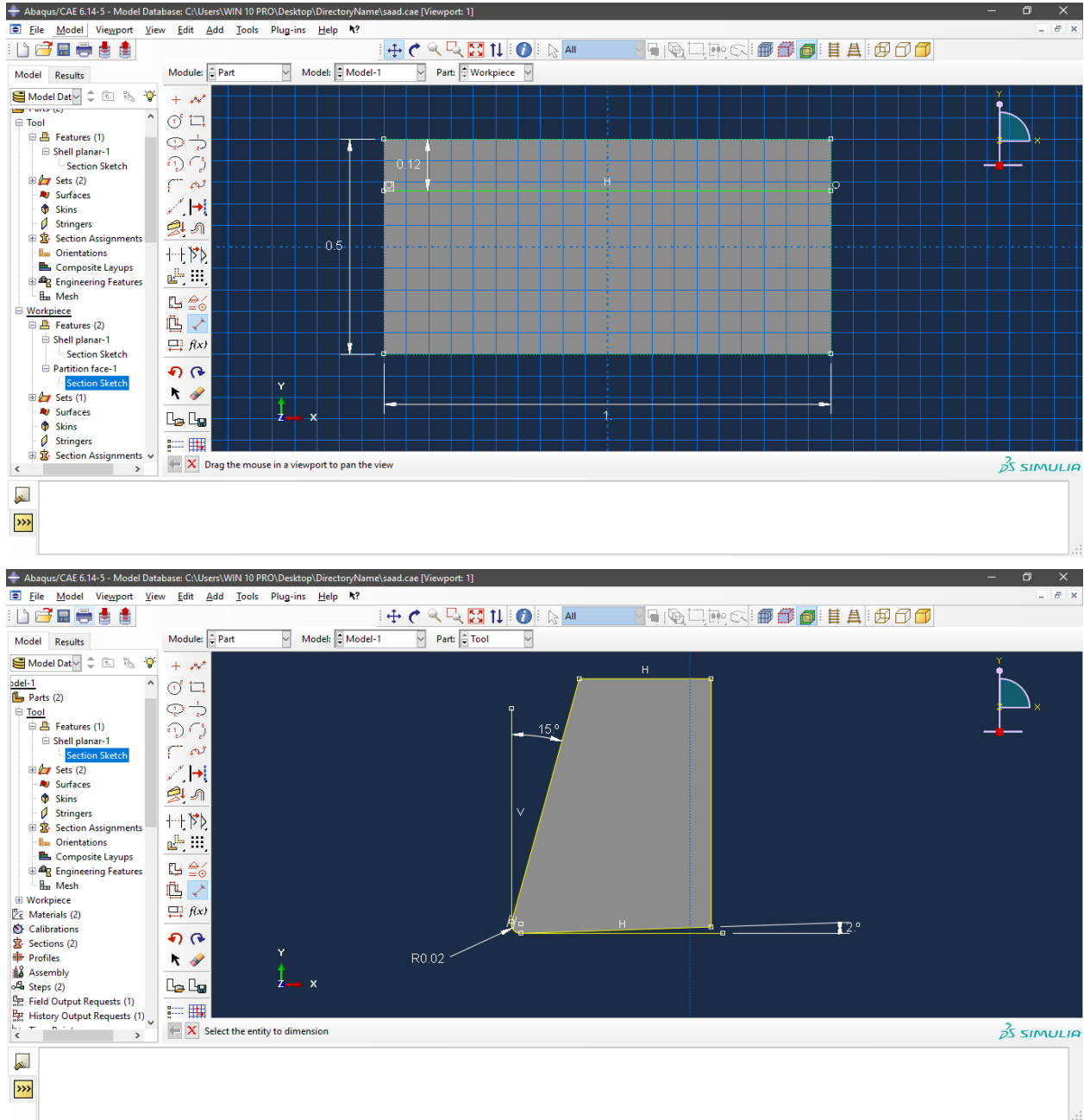


Figure 11. Geometry of the workpiece (top) and the machining tool (bottom)

The Johnson-Cook parameters for the workpiece are also assigned in the material definitions under the plasticity analysis. These parameters have been selected based on the criteria that is discussed in the later sections of this report.

3.2. Cutting Parameters Identification

Cutting parameters are crucial considerations in studying the machining of Ti₆Al₄V with a tungsten carbide tool due to their direct impact on machining efficiency, tool wear, and surface integrity of the workpiece.

The cutting speed directly affects the material removal rate and the heat generated during cutting. Ti₆Al₄V is known for its poor thermal conductivity and tendency to work-harden, making it sensitive to temperature changes. Optimizing cutting speed helps manage the heat generated at the cutting interface, minimizing tool wear and improving surface finish. Too high a cutting speed may lead to excessive tool wear, while too low a speed can cause built-up edge formation.

The uncut chip thickness influences chip formation and the forces acting on the tool. For Ti₆Al₄V, controlling chip thickness is critical to avoid chip adhesion and built-up edge formation. A thicker chip can exert higher cutting forces and increase tool wear, affecting both tool life and surface quality. Studying the relationship between chip thickness and cutting conditions aids in optimizing the machining process.

Rake and clearance angles of the cutting tool are vital for analyzing effective chip evacuation and prevention of tool-workpiece contact. The Rank Angle determines the angle of the cutting edge relative to the workpiece surface, influencing chip flow and surface finish. Meanwhile, the clearance angle ensures sufficient space for chip removal and minimizes frictional contact between the tool and workpiece, reducing heat generation and tool wear.

Similarly, the cutting-edge radius plays a significant role in tool wear and surface finish. A smaller cutting-edge radius generally improves surface quality but may increase cutting forces. For Ti₆Al₄V, selecting an appropriate cutting-edge radius balances tool life with surface integrity, crucial for achieving desired machining outcomes.

Considering these parameters in the study of Ti₆Al₄V machining with a tungsten carbide tool allows for a comprehensive understanding of the interaction between the tool, workpiece, and cutting conditions. Optimization of these parameters is essential for enhancing productivity, minimizing tool wear, and achieving superior surface finish in Ti₆Al₄V machining applications.

3.3. Cutting Model Selection (JC Model)

The selection of the Johnson-Cook (JC) material model for machining Ti₆Al₄V with a

tungsten carbide tool involves several key considerations. Ti_6Al_4V is a challenging material to machine due to its high strength, toughness, and tendency to work-harden at high temperatures. Tungsten carbide, known for its hardness and wear resistance, is a suitable choice for the cutting tool in this scenario.

The Johnson-Cook model is preferred for simulating the material behavior of Ti_6Al_4V during machining because it accurately captures its response under high strain rates and temperatures. This model incorporates parameters like strain rate sensitivity and thermal softening, crucial for predicting chip formation and tool wear. Ti_6Al_4V can experience significant thermal and mechanical loading during machining, leading to plastic deformation and chip formation. The JC model's ability to account for these factors helps in optimizing cutting parameters such as speed, feed rate, and depth of cut to enhance machining efficiency and tool life.

Furthermore, the use of tungsten carbide as the cutting tool is advantageous due to its superior hardness, thermal stability, and resistance to wear, making it suitable for cutting tough materials like Ti_6Al_4V . By employing the Johnson-Cook model alongside tungsten carbide tools, manufacturers can achieve better precision, reduce tool wear, and optimize machining strategies, ultimately improving productivity and ensuring consistent quality in the machining of Ti_6Al_4V components.

3.4. Meshing and Adaptive Meshing

The mesh settings have been selected as $10 \times 10 \mu m$ for the tool, and the machining layer of the workpiece, which is set at a reasonable value of $120 \mu m$. The mesh size at the remainder of the workpiece is set to be $100 \times 10 \mu m$ to reduce the computation time. The meshes for both components are as provided below.

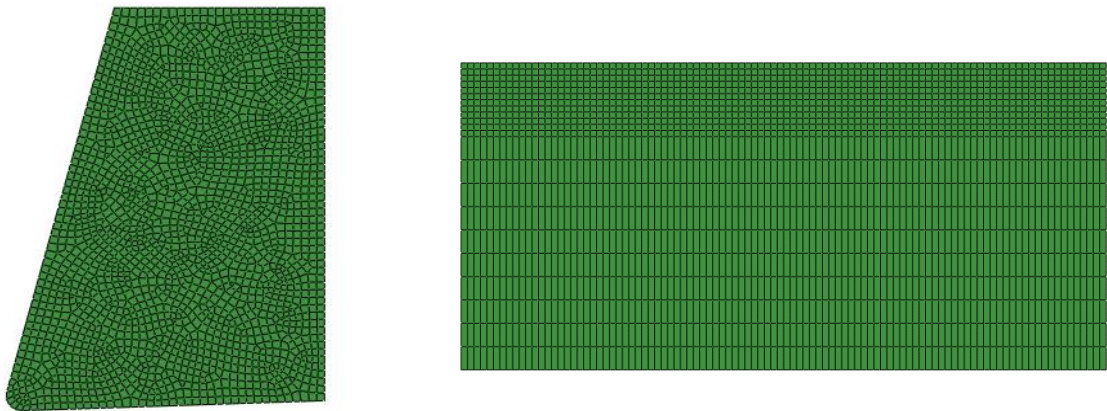


Figure 12. Mesh configuration for the machining tool (left) and the workpiece (right)

The ALE based adaptive mesh setting is selected for the study with the frequency of 10 as to reduce the computation time while providing satisfactory results. The adaptive mesh controls are also considered during the simulation.

3.5. Boundary Conditions

Since the study is based on transient motion, instead of steady state analysis, the machining step is set to be dynamic and explicit. The time step provided for the study is 0.002s which would allow for an appropriate study of time dependent effects of the machining operation on the workpiece. The workpiece and the machining tool are made to contact with one another based on kinematic contact, with a weighting factor being at the default value proposed by the software. The contact controls are also kept at default settings.

Once the contact assembly has been set on the workpiece and the tool, the encastre boundary conditions are provided to the at the bottom of the workpiece to restrict its movement in all DOFs with the velocity of 30 m/min applied on the tool as illustrated in the figure below. These conditions govern the initial positions and the motion path kinematics of the individual components. The motion approach taken for the study dictates that the workpiece remains static, while the tool moves to approach the workpiece to perform the operation. This brings convenient in dictating the machining motion since the workpiece has orthogonal dimensions while the tool has a taper and would need to incorporate additional dimension constraints in order to replicate the results. This will eventually lead to a more complex design which can pose a more strenuous computation demands.

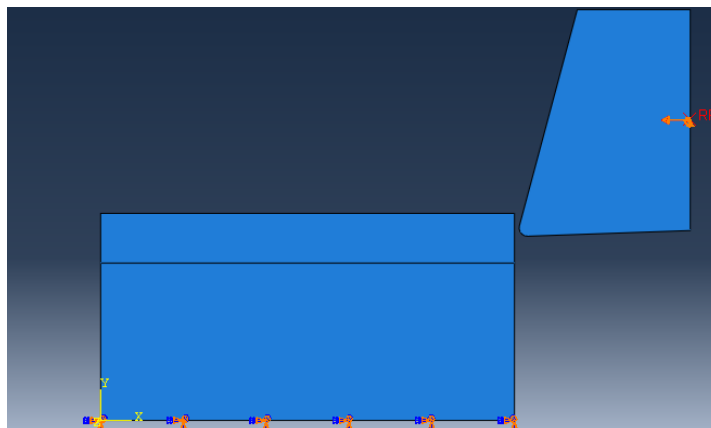


Figure 13. Boundary Constraints of Workpiece and Tool piece.

3.6. FEM Software Selection

The Finite Element Method (FEM) model employed in this study for machining Ti6Al4V was developed using ABAQUS 6.14.1. This choice was made in consideration of prior research, which served as a foundational reference for the current investigation. Utilizing ABAQUS facilitated the formulation of the workpiece and tool geometry, as well as the implementation of boundary conditions and the analysis of desired outcomes, thereby streamlining the research process.

4. CHAPTER 4: Johnson Cook Parameters for Simulation Modelling

The Johnson-Cook flow stress model (Johnson & Cook, 1983) predominates in finite element simulations of metal cutting due to its widespread use. This empirical model distinguishes plastic, viscous, and thermal effects but does not incorporate strain softening, a feature present in newer models (Ducobu F. , Arrazola, Riviere, & Filippi, 2015). However, strain softening is primarily relevant in the formation of segmented or serrated chips. As the Johnson-Cook model excels in continuous chip modeling, it remains widely adopted in current literature for its suitability in simulating machining processes where continuous chip formation is prevalent. The Johnson-Cook flow stress can be represented mathematically as

$$\sigma = (A + B\varepsilon^n) \left(1 + C \ln \frac{\dot{\varepsilon}}{\dot{\varepsilon}_o}\right) \left(1 - \left[\frac{T - T_o}{T_m - T_o}\right]^m\right)$$

This model comprises five material constants: yield strength A , hardening modulus B , strain-hardening exponent n , strain rate sensitivity C , and thermal sensitivity m . Parameters B and n govern strain hardening. T_m and T_o denote melting and room temperatures, while $\dot{\varepsilon}_o$ represents the reference strain rate. The temperature-dependent term is inactive at $T = T_m$, rendering the Johnson-Cook model unsuitable for temperatures exceeding T_m . The viscosity-related term equals 1 at $\dot{\varepsilon} = \dot{\varepsilon}_o$ which indicates flow stress independence at that specific strain rate.

4.1. Selection of JC Parameters

The parameters of the Johnson-Cook constitutive model are typically derived using Split Hopkinson Pressure Bar (SHPB) experiments. This setup enables the attainment of strains up to 0.5 and strain rates below 10^4 s^{-1} , which are lower than those encountered in machining operations. Consequently, for higher values, flow stress is extrapolated, potentially resulting in uncertain predictions. However, within the experimental range, the Johnson-Cook model accurately characterizes material behavior (Ducobu, Lorphevre, & Filippi, On the importance of the choice of the parameters of the Johnson-Cook constitutive model and their influence on the results of a Ti6Al4V orthogonal cutting model, 2017).

4.2. Evaluation of JC Parameters

The JC parameters are obtained for 32 data sets that correspond to different machining

conditions aimed to explore the chip formation and machining procedure of the titanium alloy. The JC experimental data test sets are further compared based on their stress-strain evolutions and validated with the already developed Ti6Al4V ALE Finite Element Model for 2D orthogonal cutting. The results obtained were then compared with the JC parameters based on cutting and feed forces, surface finish and chip morphology. The comparison between numerical with experimental reference outlined a basis for defining strict orthogonal cutting conditions providing the most feasible selection criteria of an optimum set of parameters of the JC constitutive model which highlight the significance of the chosen set, thus recommending the most relevant one to obtain results with higher accuracy.

5. CHAPTER 5: Orthogonal Cutting Experimentation and Simulation

The Orthogonal Cutting process of Ti6Al4V yield both experimental and simulation-based Johnson-Cook parameters test sets totaling to 32.

Understanding and utilizing these Johnson-Cook parameters are vital for optimizing cutting processes and predicting tool wear and chip formation during machining of Ti6Al4V. By leveraging this comprehensive dataset, researchers and engineers can refine their simulations and tailor machining strategies to enhance efficiency and extend tool life. Additionally, the variations observed across the test sets underscore the importance of comprehensive material characterization and the need for adaptive machining strategies to accommodate the inherent complexity of titanium alloys like Ti6Al4V in practical applications.

TABLE I: The JC Parameters Outlined for Cumulative Test Sets 1-32 respectively.

	A (MPa)	B (MPa)	C	m	n
Set 01	418.4	394.4	0.035000	1.000	0.470
Set 02	724.7	683.1	0.035000	1.000	0.470
Set 03	782.7	498.1	0.028000	1.000	0.280
Set 04	804.0	545.0	0.050000	1.040	0.362
Set 05	859.0	640.0	0.000022	1.100	0.220
Set 06	862.5	331.2	0.012000	0.800	0.340
Set 07	870.0	990.0	0.008000	1.400	1.010
Set 08	870.0	990.0	0.011000	1.000	0.250
Set 09	881.0	468.0	0.039000	0.700	0.122
Set 10	884.0	599.0	0.034000	1.040	0.362
Set 11	896.0	656.0	0.012800	0.800	0.500
Set 12	968.0	380.0	0.019700	0.577	0.431
Set 13	983.0	348.0	0.024000	0.690	0.320
Set 14	984.0	520.3	0.015000	0.824	0.510
Set 15	988.0	762.0	0.015000	1.510	0.414
Set 16	997.9	653.1	0.019800	0.700	0.450
Set 17	1080.0	1007.0	0.013040	0.770	0.598
Set 18	1098.0	1092.0	0.014000	1.100	0.930
Set 19	1104.0	1036.0	0.013900	0.779	0.635
Set 20	1119.0	838.6	0.019210	0.644	0.473
Set 21	1130.0	530.0	0.016500	0.610	0.390
Set 22	727.7	498.4	0.028000	1.000	0.280
Set 23	814.0	700.0	0.021800	0.893	0.690
Set 24	862.0	331.0	0.012000	0.800	0.340
Set 25	987.8	761.5	0.015160	1.516	0.414

Set 26	880.0	695.0	0.040000	0.800	0.360
Set 27	856.4	840.3	0.110000	0.663	0.880
Set 28	790.0	478.0	0.032000	1.000	0.280
Set 29	1000.0	780.0	0.033000	1.020	0.470
Set 30	728.7	498.4	0.028000	1.000	0.280
Set 31	889.7	683.1	0.035000	1.000	0.470
Set 32	880.0	331.0	0.012000	0.340	0.800

5.1. Experimental Set Up

The cutting conditions during orthogonal machining of Ti6Al4V are summarized and tabulated below:

TABLE II: Summarized Cutting Conditions Applied during Ti6Al4V machining process

Cutting Speed, V_c (m/min)	30
Uncut Chip Thickness, h (μm)	60
Rake Angle, γ($^\circ$)	15
Clearance Angle, α ($^\circ$)	2
Cutting Edge Radius, r (μm)	20
Mesh Size (μm)	Variable

The selected values for the cutting parameters were chosen based on their influence on the machining process and the desired outcomes when machining Ti6Al4V with a tungsten carbide tool. The cutting speed V_C was likely determined to balance between efficient material removal and minimizing tool wear. This speed is appropriate for titanium alloys like Ti6Al4V, as it helps manage heat generation during cutting, which is critical due to titanium's poor thermal conductivity.

The uncut chip thickness h ensures effective chip formation and evacuation. This thickness strikes a balance between chip control and avoiding chip adhesion on the tool edge, which can lead to poor surface finish and increased tool wear. With a rake angle γ of 15° and a clearance angle α of 2° , the tool geometry is optimized for chip flow and clearance. A smaller clearance angle helps prevent tool-workpiece contact, reducing friction and heat generation.

The cutting edge radius r facilitates a balance between achieving a smooth surface finish and minimizing cutting forces. A larger radius helps reduce the stress concentration at the cutting edge, improving tool life while maintaining surface quality. The variable Mesh Size allows for

flexibility in simulation or experimental analysis, enabling detailed modeling of the cutting process and its effects on tool wear, chip formation, and surface integrity. Together, these parameter values were carefully selected to optimize the machining process for Ti6Al4V, aiming to achieve efficient material removal with minimal tool wear and excellent surface finish.

5.1.1. Cutting and Feed Forces

The results obtained from the simulations on Ti6Al4V workpiece machining with a tungsten carbide tool, as shown by CF (cutting force) and FF (feed force), reveal interesting trends and variations across different test sets. The reported errors in force measurements and uncut chip thickness (h) with respect to experimental results highlight challenges in accurately predicting machining behavior using simulations performed in Abaqus Platform.

TABLE III: Cutting Parameters Outlined in Tabulated form for JC Test sets 1-32:

Set	CF (N)	Error (%)	FF (N)	Error (%)	h (mm)	Error (%)
Set 1	55.59	50.80	25.92	41.09	90.03	-50.05
Set 2	142.20	-25.84	67.92	-54.36	83.76	-39.6
Set 3	142.20	-25.84	67.92	-54.36	83.76	-39.6
Set 4	116.4	-3.01	68.45	-55.57	82.77	-37.95
Set 5	94.24	16.60	54.98	-24.95	75.43	-25.72
Set 6	83.10	26.46	47.18	-7.23	88.4	-47.33
Set 7	84.03	25.64	33.51	23.84	90.3	-50.5
Set 8	139.1	-23.10	74.68	-69.73	85.57	-42.62
Set 9	120.2	-6.37	80.8	-83.64	78.19	-30.32
Set 10	110.4	2.30	61.19	-39.07	78.79	-31.32
Set 11	98.29	13.02	54.25	-23.30	82.4	-37.33
Set 12	106.4	5.85	64.55	-46.70	81.73	-36.22
Set 13	107.41	4.94	63.23	-43.71	94.8	-58
Set 14	99.48	11.96	58.74	-33.51	88.97	-48.28
Set 15	139.9	-23.80	74.12	-68.45	81.6	-36
Set 16	110.46	2.24	66.19	-50.44	89.89	-49.82
Set 17	121.42	-7.45	70.37	-59.92	85.03	-41.71
Set 18	119.4	-5.66	57.89	-31.57	85.47	-42.45
Set 19	124.5	-10.18	50.37	-14.48	89.2	-48.67

Set 20	168	-48.67	92.64	-110.54	88.27	-47.12
Set 21	114.17	-1.04	73.61	-67.30	95.20	-58.66
Set 22	112.36	0.57	58.27	-32.42	85.72	-42.87
Set 23	117.96	-4.39	49.12	-11.64	95.65	-59.42
Set 24	1.01	10.75	59.63	-35.52	85.87	-43.12
Set 25	110.03	2.63	65.29	-48.39	85.97	-43.28
Set 26	122.06	-8.02	64.79	-47.26	94.82	-58.03
Set 27	192.09	-69.99	83.98	-90.86	94.82	-58.03
Set 28	98.11	13.17	52.58	-19.51	81.66	-36.11
Set 29	159.77	-41.39	89.38	-103.15	92.65	-54.42
Set 30	122.20	-8.14	74.24	-68.74	76.5	-27.5
Set 31	118.57	-4.92	59.76	-35.81	81.1	-35.17
Set 32	76.30	32.47	54.22	-23.22	83.71	-39.52

5.1.2. Chip Morphology

Chip formation during the machining process of Ti6Al4V with a tungsten carbide tool, as observed from the data provided, is influenced by various factors including material properties, cutting parameters, and tool geometry. The contour showing high stress concentrations at the tool-workpiece contact point indicates intense localized deformation and strain during cutting. As the tool engages with the workpiece, material undergoes significant plastic deformation leading to the formation of a continuous chip.

Initially, the chip formed adheres to the tool's cutting edge and progresses along with the tool's movement, resembling a continuous ribbon. However, as the machining continues, the built-up stress within the chip exceeds its structural integrity, causing it to fracture and break into smaller segments. This phenomenon is often seen in materials like Ti6Al4V, which exhibit high strength and low thermal conductivity, leading to localized heating and material softening along with the cutting zone.

Several factors contribute to chip breakage during machining. Firstly, the high cutting forces and temperatures generated during Ti6Al4V machining can induce thermal softening and increase chip brittleness, making the chip prone to fracture. Additionally, the geometry of the cutting tool, particularly the rake angle and chip breaker design, influences chip formation and evacuation. Insufficient chip space or improper tool geometry can lead to chip congestion and subsequent breakage.

Moreover, the inherent anisotropic nature of Ti6Al4V, characterized by varying

mechanical properties in different directions, can contribute to irregular chip formation and breakage. Differences in material properties across grains or phases within the alloy can create stress concentrations and discontinuities within the chip, promoting crack initiation and propagation. Understanding these mechanisms is crucial for optimizing machining parameters and tool designs to enhance chip control, minimize tool wear, and improve surface finish in Ti6Al4V machining applications.

5.2. Simulation Set Up

The simulation setup in Abaqus for the machining of Ti6Al4V with a tungsten carbide tool likely involved several key steps and considerations. Firstly, the geometry of the workpiece and tool would have been accurately modeled, incorporating the specific dimensions and material properties of both the titanium alloy and tungsten carbide. The workpiece would be defined with appropriate boundary conditions to mimic real-world machining conditions.

Next, the tool path and cutting operation would have been defined within the simulation. This involves specifying the cutting speed V_c and other relevant cutting parameters. The

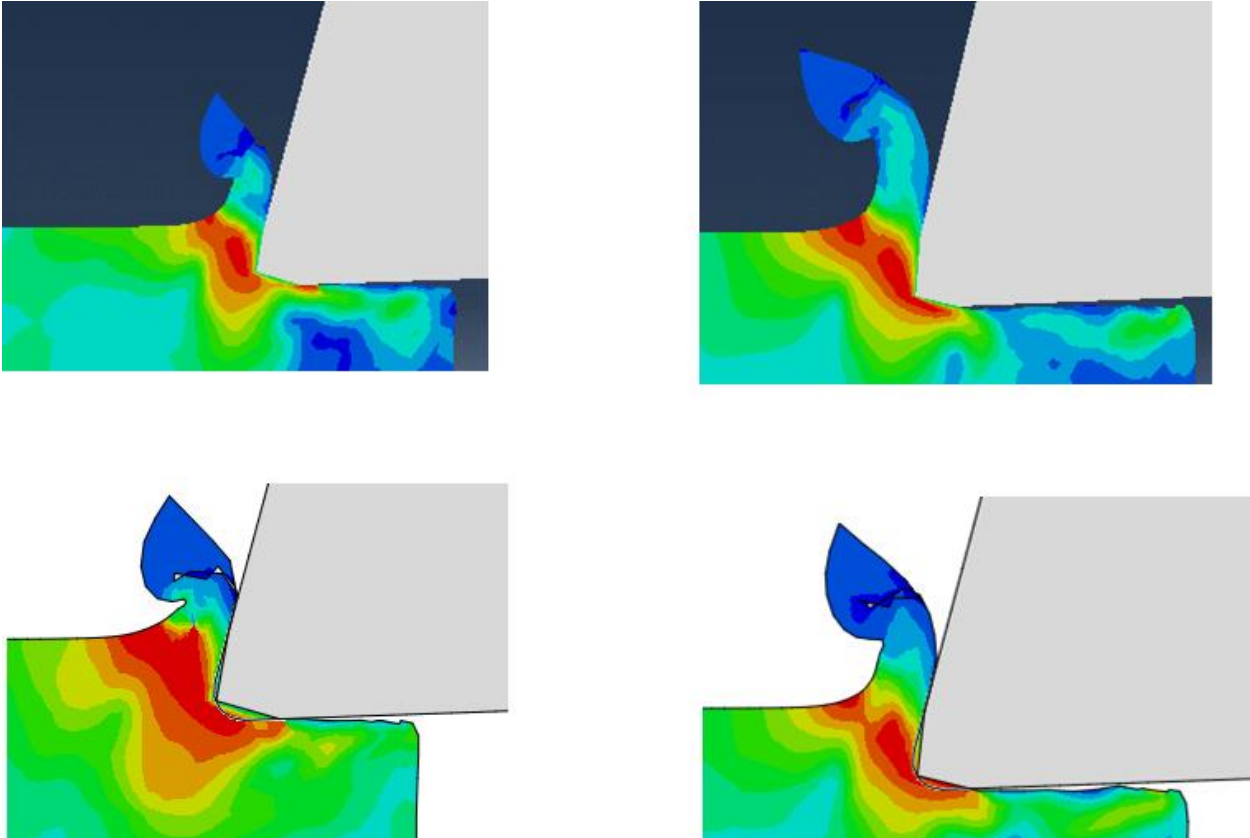


Figure 14. Von Mises Stress Contours Distribution during Orthogonal Machining of Tungsten Carbide Workpiece

interaction between the tool and workpiece, including the contact mechanics and material deformation, would be simulated using appropriate material models and element types within ABAQUS.

Meshing plays a critical role in the accuracy and stability of the simulation. The workpiece and tool would have been meshed with fine elements in the cutting region to capture the localized deformations and stresses accurately. The simulation setup would also include monitoring and analysis of cutting forces, chip formation, and other performance metrics to validate and optimize the machining process. Adjustments in mesh density, material models, or boundary conditions may be made iteratively to refine the simulation setup and improve the correlation between simulated and experimental results.

5.2.1. Finite Element Model

The finite element model (FEM) used for simulating the machining of Ti6Al4V with a tungsten carbide tool likely incorporated Johnson-Cook (JC) material parameters to capture the material behavior under high strain rates and temperatures. The JC model parameters, including A (flow stress coefficient), B (rate sensitivity coefficient), C (thermal softening parameter), m (strain hardening exponent), and n (strain rate sensitivity exponent), were calibrated based on experimental data to accurately represent Ti6Al4V's response to cutting forces and thermal effects.

The simulation aimed to replicate the actual machining process by defining cutting conditions such as cutting speed, feed rate, tool geometry, and workpiece material properties. The FEM involved meshing the workpiece and tool with appropriate element types and sizes, focusing on the tool-workpiece contact region to capture stress distribution and chip formation accurately. Simulated results, including cutting forces and chip morphology, were compared against experimental data to validate the model's predictive capability and refine the JC parameters for improved accuracy. Iterative adjustments in the FEM setup were likely performed to achieve closer agreement between simulated and experimental outcomes, ensuring reliable simulation results for optimizing machining processes.

5.2.2. Work piece Mechanical Model

The workpiece dimensions for the Ti6Al4V material in the finite element model were defined with a machining layer thickness of 120 μm . The overall mesh settings used a finer

resolution of $10 \times 10 \mu\text{m}$ for both the tool and the machining layer of the workpiece to capture detailed interactions during cutting. The remaining portion of the workpiece utilized a coarser mesh size of $100 \times 10 \mu\text{m}$ to optimize computational efficiency without compromising simulation accuracy. Adaptive meshing based on Arbitrary Lagrangian-Eulerian (ALE) techniques with a frequency of 10 was employed to dynamically refine the mesh in critical areas, such as the tool-workpiece contact region, throughout the simulation to accurately capture material deformation and chip formation while managing computation time.

5.2.3. Tool Mechanical Model

The mechanical model of the tungsten carbide tool used in the simulation included defining the tool geometry, specifically incorporating the cutting edge, rake angle, and clearance angle. The tool shape and dimensions were critical factors influencing the machining process. The defined rake angle, which dictates the inclination of the cutting edge relative to the workpiece surface, influenced chip formation and tool wear. The clearance angle, defining the angle between the tool flank and the workpiece surface, ensured proper chip evacuation and minimized frictional contact. These parameters, along with the cutting angle and tool geometry, were integrated into the finite element model to accurately simulate the tool's interaction with the Ti6Al4V workpiece during orthogonal cutting. The mechanical model of the tool played a crucial role in determining cutting forces, chip morphology, and overall machining performance in the simulation.

5.2.4. Cutting Forces Evaluation

The cutting force calculations each of the data sets involved multiple iterations to determine the Root Mean Square (RMS) values of the cutting force (CF) and resultant force (RF) across these iterations. This approach is crucial for obtaining more reliable and representative force values, especially in dynamic machining processes where forces can vary due to material heterogeneity, tool wear, or varying cutting conditions.

By conducting multiple iterations and calculating the RMS values, the simulation can account for fluctuations and variability in the cutting forces throughout the machining process. This is essential for capturing realistic force responses that may not be evident from a single simulation run. Variability in force data can arise from factors like material properties, tool geometry changes, or localized material behaviors, which are better captured and averaged out

through multiple iterations.

The RMS values provide a more stable representation of the average cutting forces and resultant forces experienced during machining. This averaging approach helps mitigate outliers or transient spikes in force data that might occur in individual simulation runs, offering a more consistent and reliable basis for analyzing machining performance and tool-workpiece interactions. Additionally, calculating RMS values over multiple iterations enhances the simulation's predictive accuracy and provides a more comprehensive understanding of the forces acting on the tool and workpiece, which is crucial for optimizing machining parameters and tool designs.

5.2.5. Chip Formation Analysis

Chip formation analysis is essential in understanding the machining process and optimizing tool performance. In the context of the simulation discussed using Abaqus for Ti6Al4V machining with a tungsten carbide tool, chip formation analysis involves studying the morphology, size, and behavior of the chips generated during cutting. This analysis provides insights into material removal mechanisms, tool wear, and surface quality.

To conduct chip formation analysis in Abaqus, post-processing tools can be utilized to visualize chip morphology and evaluate chip characteristics such as thickness, curl, and segmentation. Key steps include defining appropriate output requests during simulation to capture chip geometry and material state at critical time points. Post-processing techniques such as contour plots of chip thickness and velocity vectors can reveal dynamic chip formation processes.

Furthermore, conducting parametric studies by varying cutting parameters such as cutting speed, feed rate; or tool geometries such as rake angle, clearance angle in Abaqus simulations allows for systematic investigation of their effects on chip formation. By correlating simulation results with experimental observations, engineers can refine machining strategies, optimize tool designs, and predict chip behavior under different conditions. Ultimately, chip formation analysis aids in improving machining efficiency, reducing tool wear, and enhancing surface finish in Ti6Al4V machining processes.

5.3. Comparison between Experiment and Simulation

Comparing experimental and simulation results is essential for validating the accuracy and

reliability of computational models. Firstly, this comparison helps identify discrepancies and errors in the simulation, guiding improvements in modeling assumptions, material properties, or boundary conditions. Secondly, validating simulations against experimental data builds confidence in the predictive capabilities of the model, ensuring its suitability for real-world applications. Lastly, comparing results provides insights into underlying physical phenomena and aids in refining parameters for more accurate simulations in future studies.

5.3.1. Cutting and Feed Forces

Examining the results, set 27 stands out with notably high errors in both CF (69.989%) and FF (90.857%). This significant discrepancy suggests that the simulation for Set 27 did not adequately capture the true machining dynamics. The error percentages could be due to various factors, such as inaccurate material property inputs, insufficiently defined boundary conditions, or inappropriate modeling of the tool-workpiece interaction. Such discrepancies highlight the limitations and complexities of simulating machining processes, especially for challenging materials like Ti6Al4V.

Among the sets with more reasonable error percentages, set 28 appears to have relatively accurate results, with CF and FF errors less than 20 % and with min h error at 36.5%. This set demonstrates a closer agreement between simulation and experimental data compared to others. Similarly, sets 10,11,22 and 24 also exhibit relatively low errors in force measurements and uncut chip thickness, indicating better simulation fidelity in these cases.

The best result for CF is seen in Set 22 with an error of 0.56%, while the best result for FF is observed in Set 6 with an error of 7.22%. Similarly, the best results for h is seen in the Set 5 with the min error of 25 % The best overall result, considering both CF and FF, is likely from Set 23, with an errors of -4.3% and -11.6% which shows relatively low errors across all parameters compared to other sets.

It's worth noting that certain sets are not mentioned due to their results not converging in the Abaqus simulation, rendering the outcomes inconclusive. This lack of convergence could stem from several issues, including inadequate mesh refinement, improper element types or sizes, numerical instability, or unrealistic boundary conditions. The complex interaction between the tungsten carbide tool and Ti6Al4V workpiece, characterized by high cutting forces and material properties, necessitates meticulous modeling and parameter calibration for accurate simulation

outcomes.

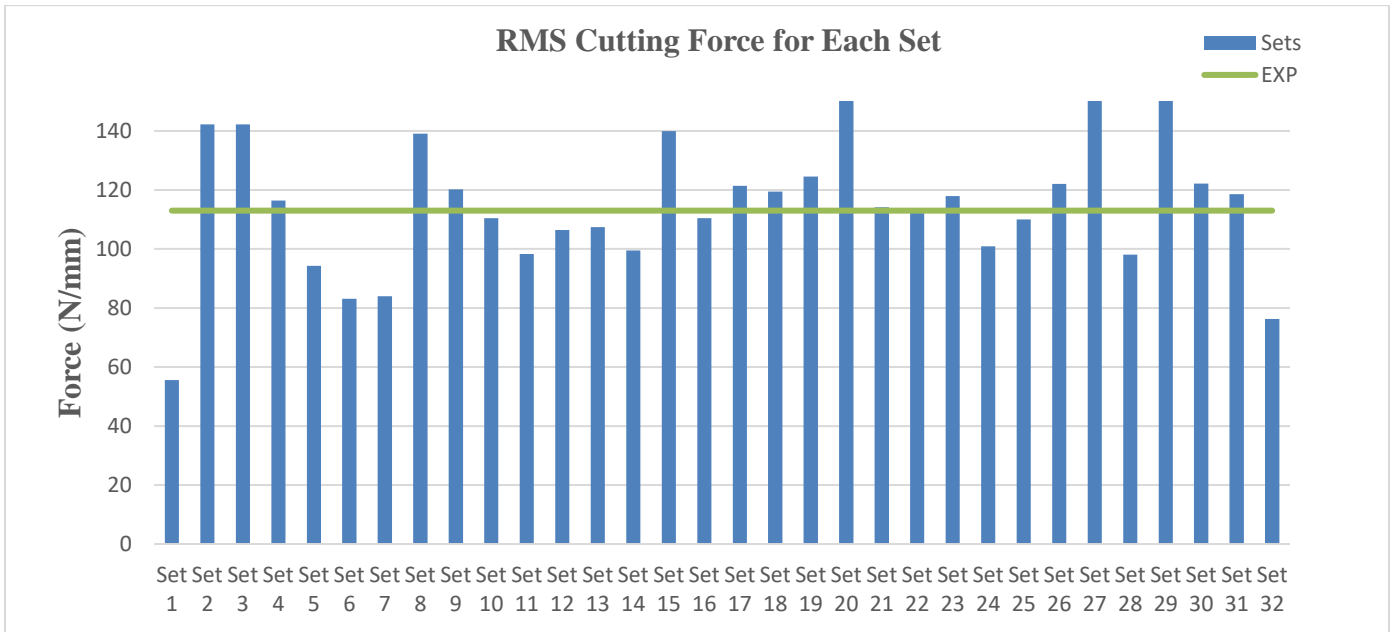


Figure 15. RMS vs Cutting Force for Each Set

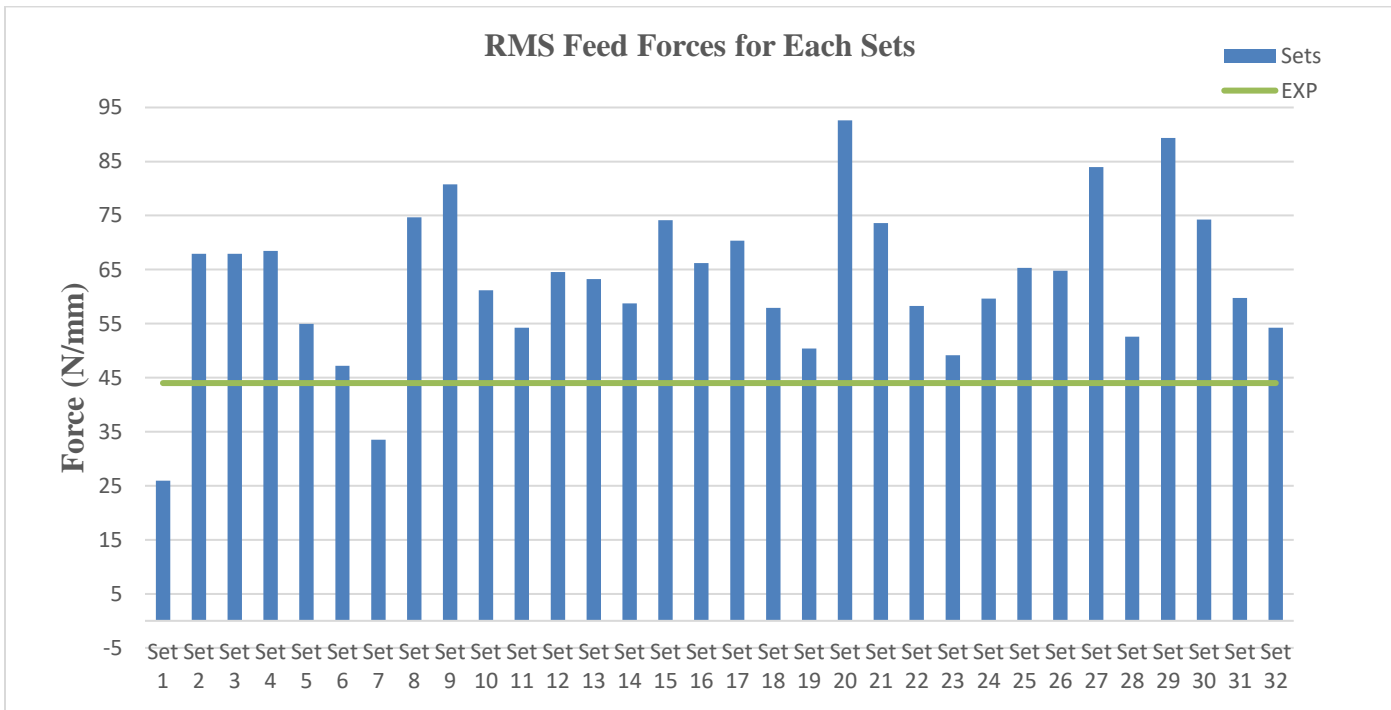


Figure 16. RMS Feed Force for Each Set

5.3.2. Chip Formation

Comparing simulation and experimental chip formation based on the provided data is

crucial for evaluating the predictive accuracy of the simulation model. By analyzing chip morphology, thickness, and segmentation from both simulation and experimental results, engineers can assess how well the simulated machining process replicates real-world behavior. Discrepancies between the two sets of data can highlight areas where the simulation may need refinement, such as adjusting material parameters or optimizing mesh settings to better capture chip formation dynamics.

Moreover, comparing simulation and experimental chip formation allows for a deeper understanding of the underlying mechanisms driving chip morphology. Insights gained from this comparison can inform improvements in tool design, cutting parameters, and process optimization strategies. Overall, this analysis facilitates the development of more reliable and effective simulation models for predicting chip formation in Ti6Al4V machining, ultimately leading to enhanced machining efficiency and quality.

5.4. Discussion

The plotted von Mises stress data for selected sets across varying time intervals reveals important insights into the material behavior during machining of Ti6Al4V using a tungsten carbide tool. Notable trends can be observed in how stress levels evolve over time, shedding light on the effectiveness of the machining process and potential areas of concern.

Initially, the data shows that as machining progresses (increasing time on the x-axis), von Mises stress generally exhibits fluctuations but tends to stabilize around certain levels. This stabilization suggests a steady-state condition in the material response under sustained cutting conditions. Sets with higher Johnson-Cook (JC) material parameters, such as higher values of A (flow stress coefficient) and B (rate sensitivity coefficient), might exhibit higher stress levels due to increased material strength and sensitivity to strain rate and temperature.

Anomalies in stress levels could indicate localized material behaviors, such as chip formation or tool-workpiece interactions. For instance, spikes in stress observed at specific time points might correspond to critical stages in chip formation where material undergoes rapid deformation and strain. Understanding these stress variations is crucial for optimizing machining parameters to minimize stress concentrations and prevent premature tool wear.

Comparing stress levels across different sets allows for evaluating the impact of varying cutting conditions and tool geometries on material response. Sets with lower stress levels over time

may indicate more efficient material removal and reduced energy dissipation, suggesting optimal machining conditions. Conversely, sets with persistent high stress levels may necessitate adjustments in cutting parameters to enhance process stability and tool longevity.

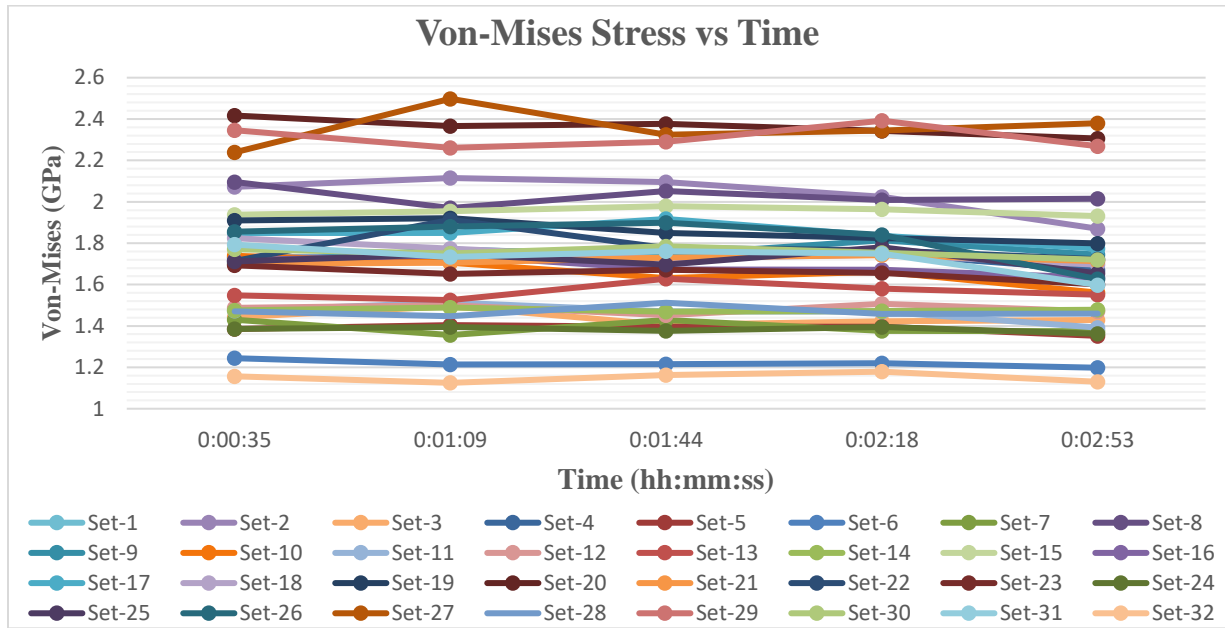


Figure 17. Graphical Analysis outlining Von Mises Stress produced during TiGAL4V machining vs Machining Time

5.4.1. Impact of Chip Morphology on Material Surface Finish and Tool Life

The morphology of chips produced during machining plays a critical role in influencing both material surface finish and tool life. Chip morphology refers to the shape, size, and characteristics of the chips generated during the cutting process. Understanding the impact of chip morphology is essential for optimizing machining processes and enhancing overall productivity.

Firstly, chip morphology directly affects material surface finish. The presence of continuous, well-formed chips with consistent thickness and minimal segmentation often correlates with smoother surface finishes on machined parts. Conversely, irregular or discontinuous chips can lead to surface imperfections, such as chatter marks or surface roughness. Therefore, controlling chip morphology through appropriate cutting parameters and tool designs is crucial for achieving desired surface quality in machining operations.

Secondly, chip morphology influences tool life by affecting chip-tool interactions. Proper chip formation can help facilitate efficient chip evacuation, reducing heat generation and friction at the tool-chip interface. This, in turn, minimizes tool wear and prolongs tool life. On the other hand, inadequate chip control, such as chip jamming or built-up edge formation, can accelerate

tool wear and compromise machining performance. Optimizing chip morphology can significantly enhance tool life and reduce overall manufacturing costs by minimizing tool replacement and maintenance.

Furthermore, chip morphology impacts chip recycling and material utilization in machining processes. Well-formed chips are easier to collect and recycle, contributing to sustainable manufacturing practices. Additionally, understanding chip morphology allows for predictive modeling of machining processes, enabling engineers to optimize cutting strategies for specific materials and applications. By focusing on chip control and morphology, manufacturers can improve surface quality, extend tool life, and promote more efficient and sustainable machining practices in various industries, from aerospace to automotive manufacturing.

5.4.2. Impact of Cutting Forces on Material Surface Finish and Tool Life

The impact of cutting forces on material surface finish and tool life is significant in machining processes, particularly when dealing with materials like Ti6Al4V and utilizing tungsten carbide tools. Cutting forces, influenced by Johnson-Cook (JC) material parameters, tool dimensions, and von Mises stresses, directly affect surface quality and tool performance.

Firstly, higher cutting forces, characterized by elevated values of A (flow stress coefficient) and B (rate sensitivity coefficient) in the JC model, can lead to increased material deformation and tool wear. Excessive forces result in higher frictional heat generation and tool contact pressures, potentially causing surface irregularities and reduced finish quality.

Moreover, cutting forces impact tool life by contributing to wear mechanisms such as abrasion, adhesion, and thermal degradation. Tools experiencing prolonged exposure to high cutting forces, as indicated by von Mises stress data, are more susceptible to premature wear and failure. Understanding the relationship between cutting forces and tool life is crucial for optimizing tool materials, geometries, and coatings to enhance durability and performance.

Analyzing experimental and simulation data on cutting forces enables engineers to optimize machining parameters for improved surface finish and extended tool life. By correlating cutting force magnitudes with surface roughness measurements and tool wear rates, researchers can identify optimal operating conditions that minimize forces while maintaining productivity. This approach facilitates the development of robust machining strategies tailored to maximize efficiency and reduce costs in machining Ti6Al4V components with tungsten carbide tools.

5.4.3. Impact of Mesh Density on Accuracy of Model

The impact of mesh density on the accuracy of finite element models is crucial for ensuring reliable simulations, especially in machining simulations involving Ti6Al4V and tungsten carbide tools. The chosen mesh settings, including a finer resolution of $10 \times 10 \mu\text{m}$ for the tool and machining layer of the workpiece, with a coarser mesh size of $100 \times 10 \mu\text{m}$ for the remainder of the workpiece, are designed to balance computational efficiency with simulation accuracy.

Increasing mesh density, particularly in critical areas like the tool-workpiece contact region, can enhance the accuracy of stress and strain predictions by capturing localized deformation more effectively. This finer mesh resolution allows for better representation of material behaviors under dynamic loading conditions, such as during cutting operations. Conversely, reducing mesh density in less critical areas helps optimize computational resources without significantly compromising simulation fidelity.

The use of adaptive meshing with a frequency of 10 further improves simulation efficiency by dynamically refining the mesh in response to changing material states and deformation patterns during machining. Adaptive mesh controls ensure that the simulation maintains accuracy while minimizing computational overhead. However, it's important to note that excessively fine meshing throughout the entire model can lead to increased computational costs and potential numerical instability, especially for large-scale simulations.

6. CHAPTER 6: Conclusions and Future Recommendations

The analysis covered various aspects of simulating Ti6Al4V machining with a tungsten carbide tool using Abaqus. Key parameters included Johnson-Cook material constants for Ti6Al4V, tool geometry (rake and clearance angles), cutting forces, chip formation, von Mises stresses, and mesh settings. The discussion highlighted the importance of accurate simulation in optimizing cutting conditions, understanding chip morphology's impact, and evaluating tool performance based on cutting forces and mesh density adjustments. Integrating experimental data with simulation results enhances process understanding and optimization.

6.1. Conclusions

The comprehensive analysis and simulation of Ti6Al4V machining with a tungsten carbide tool using Abaqus have provided valuable insights into optimizing cutting processes. By incorporating Johnson-Cook material parameters, tool geometry details (rake and clearance angles), and considering cutting forces, chip morphology, von Mises stresses, and mesh settings, a holistic understanding of machining dynamics was achieved. The study underscores the significance of accurate simulation in refining machining strategies, enhancing surface finish, and extending tool life. Integrating experimental data with simulation results enables informed decision-making, guiding process improvements and tool design optimizations. This research contributes to advancing machining technologies, ensuring efficiency, reliability, and quality in aerospace and engineering applications involving challenging materials like Ti6Al4V.

6.2. Future Recommendations

Looking ahead, future research in the area of Ti6Al4V machining with tungsten carbide tools using Abaqus simulations should focus on several key areas to further enhance understanding and optimize machining processes. Firstly, investigating the influence of additional cutting parameters, such as tool wear and lubrication conditions, would provide a more comprehensive analysis of machining dynamics. Exploring the interaction between tool wear and material deformation over extended machining durations could reveal critical insights into tool life prediction and process stability.

Furthermore, integrating advanced material modeling techniques, such as incorporating

temperature-dependent material properties and strain rate effects, would enhance the accuracy and predictive capability of simulations. This would allow for more realistic representation of Ti6Al4V's behavior under varying machining conditions, particularly at elevated temperatures and high strain rates experienced during cutting processes.

Lastly, future studies could explore multi-physics simulations that couple thermal, mechanical, and material deformation aspects to capture complex phenomena like thermal softening and chip-tool interactions more accurately. By integrating these aspects, researchers can develop sophisticated machining models that enable precise optimization of cutting parameters, leading to improved surface finish, reduced tool wear, and enhanced machining efficiency in aerospace and manufacturing applications involving titanium alloys. These advancements will contribute to advancing the state-of-the-art in machining simulation technologies, supporting industry efforts towards sustainable and high-performance machining processes.

APPENDIX

Below provided are the calculations conducted for force evaluation for each data set over 20 iterations for all cases. The RMS values of the iterations are then recorded to account for unidirectional variations.

SET 01				SET 02			
CF	CF ²	RF	RF ²	CF	CF ²	RF	RF ²
-59.802	3576.219	-26.885	722.792	-155.918	24310.423	-52.511	2757.384
-47.018	2210.692	-55.661	3098.125	-126.077	15895.410	-68.482	4689.730
-63.395	4018.964	-36.644	1342.775	-145.519	21175.779	-45.461	2066.721
-16.614	276.018	-0.199	0.039	-130.956	17149.474	-37.311	1392.088
-57.593	3316.988	-11.721	137.375	-163.116	26606.829	-92.590	8572.964
-51.825	2685.841	-18.819	354.151	-168.687	28455.304	-79.702	6352.473
-62.763	3939.169	-17.855	318.794	-176.505	31154.015	-55.636	3095.387
-61.030	3724.685	-5.935	35.225	-100.264	10052.870	-62.538	3911.039
-63.100	3981.623	-17.127	293.344	-165.460	27377.012	-60.892	3707.811
-38.280	1465.366	-4.689	21.988	-172.081	29611.871	-79.148	6264.374
-67.598	4569.503	-25.687	659.796	-145.649	21213.631	-82.797	6855.327
-66.751	4455.629	-26.566	705.758	-156.012	24339.744	-82.481	6803.066
-74.761	5589.252	-22.576	509.667	-157.668	24859.198	-62.257	3875.884
-68.574	4702.393	-25.783	664.784	-153.628	23601.562	-58.037	3368.259
-25.184	634.214	-30.697	942.300	-151.058	22818.519	-85.786	7359.152
-64.187	4119.997	-34.624	1198.821	-143.768	20669.238	-53.985	2914.380
-61.633	3798.577	-21.529	463.506	-118.530	14049.361	-66.474	4418.739
-47.668	2272.276	-29.420	865.531	-98.071	9617.980	-113.560	12895.874
-38.820	1506.969	-33.111	1096.305	-99.057	9812.289	-12.542	157.302
-31.349	982.772	-2.202	4.849	-40.924	1674.807	-28.263	798.786
	3091.357		671.796		20222.266		4612.837
	55.600		25.919		142.205		67.918

SET 03				SET 04			
CF	CF ²	RF	RF ²	CF	CF ²	RF	RF ²
-155.918	24310.423	-52.511	2757.384	-122.329	14964.384	-44.764	2003.852
-126.077	15895.410	-68.482	4689.730	-98.008	9605.490	-79.072	6252.318
-145.519	21175.779	-45.461	2066.721	-111.903	12522.281	-32.326	1044.944
-130.956	17149.474	-37.311	1392.088	-116.383	13545.003	-63.880	4080.680
-163.116	26606.829	-92.590	8572.964	-104.435	10906.669	-88.793	7884.232
-168.687	28455.304	-79.702	6352.473	-101.247	10250.955	-91.163	8310.656

-176.505	31154.015	-55.636	3095.387	-132.197	17476.047	-95.061	9036.594
-100.264	10052.870	-62.538	3911.039	-123.192	15176.269	-50.158	2515.835
-165.460	27377.012	-60.892	3707.811	-129.642	16807.048	-80.483	6477.465
-172.081	29611.871	-79.148	6264.374	-133.949	17942.335	-62.566	3914.542
-145.649	21213.631	-82.797	6855.327	-102.089	10422.164	-73.816	5448.831
-156.012	24339.744	-82.481	6803.066	-130.714	17086.150	-63.636	4049.540
-157.668	24859.198	-62.257	3875.884	-119.433	14264.241	-62.546	3912.027
-153.628	23601.562	-58.037	3368.259	-133.462	17812.105	-79.820	6371.280
-151.058	22818.519	-85.786	7359.152	-157.863	24920.727	-78.198	6114.943
-143.768	20669.238	-53.985	2914.380	-117.193	13734.199	-65.599	4303.242
-118.530	14049.361	-66.474	4418.739	-118.299	13994.653	-65.781	4327.100
-98.071	9617.980	-113.560	12895.874	-104.634	10948.274	-41.991	1763.210
-99.057	9812.289	-12.542	157.302	-71.702	5141.191	-76.798	5897.871
-40.924	1674.807	-28.263	798.786	-71.631	5130.943	-1.427	2.037
	20222.266		4612.837		13632.556		4685.560
	142.205		67.918		116.759		68.451

SET 05

SET 06

CF	CF²	RF	RF²	CF	CF	CF²	RF
-72.739	5290.991	-19.813	392.571	-64.290	-109.921	12082.626	-37.257
-78.409	6147.987	-79.639	6342.338	-66.122	-93.508	8743.653	-48.371
-34.614	1198.094	-26.233	688.181	-80.955	-78.486	6160.052	-46.441
-77.236	5965.446	-33.008	1089.548	-71.513	-56.409	3181.998	-20.191
-90.882	8259.502	-12.753	162.631	-55.816	-57.601	3317.818	-1.243
-85.582	7324.210	-48.131	2316.593	-73.659	-94.764	8980.140	-13.116
-69.752	4865.328	-22.839	521.606	-86.425	-56.941	3242.323	1.055
-113.864	12965.010	-64.766	4194.674	-90.815	-83.109	6907.039	-19.768
-117.190	13733.496	-55.426	3072.008	-97.662	-90.878	8258.884	-19.278
-111.940	12530.564	-79.976	6396.161	-88.894	-93.295	8703.882	-19.799
-121.249	14701.320	-63.272	4003.333	-97.767	-98.314	9665.623	-16.756
-112.134	12574.034	-54.112	2928.109	-87.260	-97.726	9550.352	-18.607
-132.864	17652.842	-102.803	10568.457	-98.783	-99.619	9923.945	-34.472
-100.633	10127.001	-45.648	2083.731	-98.583	-82.186	6754.456	-18.101
-90.381	8168.689	-51.127	2613.970	-95.681	-65.670	4312.496	-55.518
-109.059	11893.865	-60.160	3619.226	-106.195	-101.912	10386.056	-35.709
-103.822	10779.008	-48.000	2303.952	-90.485	-90.947	8271.393	-40.935
-88.888	7901.059	-69.208	4789.706	-74.753	-72.901	5314.527	-74.318
-56.243	3163.219	-52.011	2705.144	-54.807	-75.480	5697.245	-27.770
-48.679	2369.684	-7.430	55.200	-48.804	-41.969	1761.355	-19.085
	8880.567		3042.357			7060.793	

94.237

55.158

84.029

SET 07

SET 08

RF ²	CF ²	RF	RF ²	CF	CF ²	RF	RF ²
1388.106	4133.256	-10.693	114.342	-134.591	18114.737	-55.211	3048.210
2339.773	4372.119	-67.431	4546.994	-128.801	16589.698	-46.101	2125.339
2156.776	6553.696	-67.240	4521.150	-30.249	914.972	0.270	0.073
407.681	5114.138	-9.982	99.631	-109.233	11931.848	-15.747	247.968
1.546	3115.404	-11.159	124.530	-124.994	15623.500	-77.747	6044.658
172.016	5425.692	-23.041	530.897	-146.583	21486.576	-55.342	3062.759
1.114	7469.194	-55.857	3119.960	-179.214	32117.658	-87.741	7698.501
390.790	8247.437	-54.529	2973.434	-121.237	14698.410	-57.128	3263.654
371.653	9537.886	-60.956	3715.610	-178.362	31813.003	-86.921	7555.208
391.996	7902.072	-55.130	3039.317	-152.580	23280.656	-72.794	5298.923
280.777	9558.386	-58.135	3379.701	-180.998	32760.276	-98.162	9635.857
346.206	7614.377	-38.319	1468.369	-160.168	25653.788	-85.315	7278.700
1188.346	9758.022	-44.092	1944.104	-124.924	15606.006	-100.580	10116.336
327.657	9718.628	-51.863	2689.781	-176.265	31069.350	-125.943	15861.639
3082.248	9154.777	-54.357	2954.727	-135.251	18292.833	-55.543	3085.025
1275.126	11277.378	-53.942	2909.783	-158.042	24977.274	-88.726	7872.356
1675.666	8187.590	-54.482	2968.299	-164.435	27038.869	-96.923	9394.010
5523.225	5588.041	-35.138	1234.651	-111.871	12515.121	-56.693	3214.040
771.167	3003.763	-46.266	2140.580	-80.165	6426.379	-81.886	6705.350
364.237	2381.811	6.702	44.916	-76.201	5806.516	-5.552	30.820
1122.805	6905.683		2226.039		19335.874		5576.971
33.508	83.100		47.181		139.053		74.679

SET 9

SET 10

CF	CF ²	RF	RF ²	CF	CF ²	RF	RF ²
-89.308	7975.830	-16.195	262.268	-99.434	9887.180	-34.560	1194.394
-90.121	8121.723	-90.451	8181.293	-121.923	14865.218	-47.260	2233.536
-100.473	10094.824	-95.258	9074.048	-127.359	16220.315	-84.298	7106.136
-104.315	10881.619	-27.798	772.707	-107.822	11625.584	-65.333	4268.414
-83.853	7031.359	-48.492	2351.435	-112.414	12636.907	-18.116	328.204
-114.474	13104.297	-62.813	3945.486	-90.726	8231.189	-112.257	12601.634
-130.538	17040.169	-68.972	4757.123	-80.288	6446.131	-31.022	962.364
-142.583	20329.912	-85.634	7333.148	-116.972	13682.449	-69.801	4872.138
-128.075	16403.206	-96.194	9253.266	-84.498	7139.895	-35.500	1260.278
-111.796	12498.346	-60.516	3662.186	-117.420	13787.456	-70.009	4901.288
-106.220	11282.688	-54.548	2975.462	-111.098	12342.766	-9.662	93.348

-144.829	20975.439	-150.279	22583.778	-127.192	16177.805	-67.941	4615.939
-132.224	17483.186	-76.010	5777.520	-137.795	18987.462	-59.748	3569.788
-135.924	18475.334	-85.669	7339.092	-131.286	17236.014	-74.566	5560.059
-158.276	25051.292	-107.962	11655.793	-117.198	13735.371	-57.535	3310.322
-194.087	37669.764	-121.082	14660.851	-132.393	17527.906	-94.711	8970.079
-117.934	13908.428	-68.057	4631.755	-125.872	15843.760	-46.243	2138.406
-92.156	8492.747	-98.038	9611.489	-93.820	8802.174	-66.647	4441.783
-87.681	7687.975	-44.535	1983.331	-82.085	6737.947	-48.381	2340.673
-67.114	4504.329	2.887	8.335	-41.020	1682.632	-11.065	122.441
	14450.623		6541.018		12179.808		3744.561
	120.211		80.877		110.362		61.193

SET 11

SET 12

CF	CF ²	RF	RF ²	CF	CF ²	RF	RF ²
-98.700	9741.710	-43.643	1904.711	-82.821	6859.368	-28.081	788.559
-86.876	7547.353	-29.299	858.402	-114.914	13205.227	-53.078	2817.242
-89.782	8060.772	-46.775	2187.863	-112.323	12616.456	-58.921	3471.731
-85.185	7256.467	-25.239	637.027	-46.555	2167.349	-4.239	17.965
-101.517	10305.701	-58.070	3372.078	-78.373	6142.296	-30.119	907.160
-106.344	11309.046	-62.988	3967.539	-87.266	7615.407	-40.427	1634.334
-116.088	13476.424	-64.990	4223.726	-134.860	18187.220	-105.365	11101.783
-110.484	12206.714	-53.564	2869.049	-126.140	15911.300	-85.543	7317.571
-112.753	12713.239	-71.421	5100.959	-119.342	14242.513	-88.739	7874.610
-99.811	9962.296	-49.442	2444.462	-135.050	18238.503	-79.250	6280.578
-124.184	15421.666	-75.803	5746.125	-129.818	16852.713	-71.238	5074.881
-104.754	10973.401	-64.284	4132.394	-105.669	11165.938	-56.108	3148.052
-106.870	11421.197	-72.396	5241.195	-168.938	28540.048	-129.817	16852.453
-107.006	11450.284	-56.981	3246.812	-76.037	5781.595	-36.584	1338.382
-110.502	12210.692	-57.248	3277.368	-107.821	11625.368	-47.603	2266.084
-99.297	9859.835	-44.518	1981.870	-113.816	12954.082	-52.243	2729.362
-82.534	6811.845	-70.352	4949.418	-81.655	6667.572	-64.692	4185.068
-85.877	7374.790	-36.674	1344.968	-89.678	8042.180	-51.801	2683.313
-64.070	4104.901	-35.912	1289.650	-74.712	5581.943	-53.268	2837.490
-31.578	997.157	-9.410	88.556	-63.432	4023.644	4.460	19.896
	9660.274		2943.209		11321.036		4167.326
	98.287		54.251		106.400		64.555

SET 13

SET 14

CF	CF ²	RF	RF ²	CF	CF ²	RF	RF ²
-85.281	7272.798	-31.675	1003.331	-78.366	6141.214	-36.208	1310.998

-98.128	9629.124	-90.386	8169.593	-105.674	11166.994	-79.497	6319.837
-105.027	11030.671	-56.493	3191.425	-107.067	11463.342	-86.157	7423.046
-109.680	12029.702	-48.463	2348.614	-28.882	834.187	-31.497	992.080
-102.555	10517.528	-46.135	2128.429	-1.554	2.414	-1.034	1.070
-115.001	13225.230	-75.981	5773.158	-88.377	7810.423	-38.991	1520.329
-57.379	3292.327	-29.573	874.545	-90.560	8201.168	-20.925	437.843
-128.307	16462.686	-67.668	4578.891	-133.846	17914.752	-65.268	4259.847
-122.747	15066.826	-75.766	5740.472	-105.024	11030.041	-51.661	2668.818
-74.328	5524.577	-38.398	1474.422	-120.675	14562.456	-67.082	4499.941
-167.694	28121.278	-96.992	9407.506	-131.988	17420.832	-73.246	5364.962
-106.882	11423.762	-52.724	2779.852	-120.743	14578.872	-64.753	4193.003
-45.554	2075.167	7.400	54.756	-119.585	14300.572	-65.449	4283.532
-156.614	24527.945	-102.778	10563.317	-133.901	17929.478	-77.803	6053.291
-132.803	17636.637	-75.383	5682.627	-120.154	14436.984	-93.597	8760.455
-133.826	17909.398	-83.146	6913.191	-58.518	3424.345	-29.472	868.622
-104.975	11019.751	-38.973	1518.879	-122.175	14926.731	-62.567	3914.617
-71.791	5153.876	-58.134	3379.527	-79.669	6347.165	-51.406	2642.608
-71.315	5085.872	-66.111	4370.664	-61.979	3841.446	-51.742	2677.183
-61.209	3746.529	4.054	16.437	-40.059	1604.748	-28.685	822.852
	11537.584		3998.482		9896.908		3450.747
	107.413		63.234		99.483		58.743

SET 15

SET 16

CF	CF ²	RF	RF ²	CF	CF ²	RF	RF ²
-141.119	19914.572	-47.704	2275.691	-106.485	11339.055	-42.923	1842.418
-129.450	16757.303	-58.100	3375.645	-90.453	8181.745	-60.196	3623.595
-134.298	18035.953	-64.532	4164.340	-100.134	10026.818	-30.371	922.398
-133.281	17763.825	-58.776	3454.665	-37.460	1403.259	-4.333	18.775
-138.863	19282.933	-36.649	1343.113	-79.124	6260.639	-12.554	157.595
-144.893	20993.981	-53.397	2851.240	-130.518	17034.948	-63.839	4075.469
-166.621	27762.558	-86.786	7531.775	-133.401	17795.827	-57.965	3359.895
-162.669	26461.204	-83.462	6965.889	-167.639	28102.834	-110.841	12285.727
-161.475	26074.176	-105.341	11096.726	-120.201	14448.280	-75.609	5716.691
-154.191	23774.864	-76.470	5847.676	-142.163	20210.319	-80.076	6412.230
-143.848	20692.247	-74.673	5575.997	-140.084	19623.527	-76.943	5920.179
-149.312	22294.073	-109.329	11952.830	-128.211	16438.061	-89.987	8097.660
-159.634	25483.014	-82.669	6834.130	-135.720	18419.918	-79.588	6334.313
-134.610	18119.852	-75.918	5763.512	-134.837	18181.017	-68.884	4745.019
-138.225	19106.151	-68.204	4651.731	-56.775	3223.435	-17.406	302.976
-158.758	25204.103	-80.195	6431.174	-87.178	7600.021	-80.051	6408.163

-138.706	19239.354	-44.649	1993.524	-90.880	8259.156	-75.209	5656.409
-115.110	13250.312	-71.456	5105.903	-88.444	7822.253	-93.280	8701.065
-81.203	6593.976	-112.326	12617.130	-77.810	6054.458	-51.975	2701.432
-69.140	4780.298	-6.139	37.682	-60.341	3641.060	-18.855	355.515
	19579.237		5493.519		12203.332		4381.876
	139.926		74.118		110.469		66.196

SET 17

SET 18

CF	CF ²	RF	RF ²	CF	CF ²	RF	RF ²
-140.32	19689.14	-45.26	2048.81	-141.738	20089.661	-47.572	2263.076
-99.90	9979.27	-87.66	7683.61	-108.205	11708.322	-47.220	2229.700
-103.50	10712.87	-91.70	8409.73	-118.323	14000.332	-58.024	3366.773
-134.01	17957.34	-77.96	6077.78	-112.171	12582.333	-25.261	638.128
-90.40	8171.49	-13.14	172.62	-96.975	9404.228	-9.970	99.407
-155.78	24268.34	-97.34	9475.06	-121.381	14733.347	-17.380	302.061
-101.90	10384.02	-37.39	1398.11	-143.018	20454.148	-67.225	4519.228
-124.13	15407.51	-73.37	5382.88	-133.378	17789.691	-59.171	3501.207
-107.30	11513.08	-57.61	3319.23	-116.322	13530.808	-52.041	2708.255
-159.96	25586.56	-65.12	4240.13	-119.575	14298.181	-111.240	12374.338
-135.36	18323.41	-72.62	5273.46	-117.223	13741.232	-46.172	2131.817
-157.65	24852.26	-108.89	11855.94	-146.549	21476.609	-63.369	4015.630
-141.42	19999.33	-116.37	13542.21	-152.560	23274.554	-58.722	3448.250
-67.43	4546.67	10.50	110.30	-140.256	19671.746	-49.704	2470.478
-140.01	19602.80	-63.35	4013.70	-134.998	18224.460	-49.196	2420.286
-137.98	19038.76	-61.40	3770.08	-89.150	7947.794	-25.409	645.622
-135.14	18261.47	-60.73	3687.66	-111.898	12521.162	-109.382	11964.422
-74.98	5622.23	-33.16	1099.36	-90.335	8160.484	-84.873	7203.409
-87.18	7600.61	-85.33	7280.39	-90.342	8161.749	-15.745	247.911
-57.86	3347.73	-13.68	187.01	-58.572	3430.644	-20.788	432.141
	14743.24		4951.40		14260.074		3349.107
	121.42		70.37		119.416		57.871

SET 19

SET 20

CF	CF ²	RF	RF ²	CF	CF ²	RF	RF ²
-145.131	21063.007	-47.673	2272.696	-178.859	31990.542	-58.415	3412.289
-135.982	18491.104	-46.568	2168.569	-158.057	24982.015	-80.705	6513.232
-122.130	14915.737	-57.082	3258.400	-106.892	11425.900	-111.220	12369.888
-72.099	5198.237	-1.612	2.599	-130.288	16974.963	-14.677	215.406
-130.051	16913.263	-18.181	330.534	-176.193	31043.973	-76.751	5890.655
-124.398	15474.862	-19.986	399.452	-208.220	43355.568	-96.248	9263.716

-98.750	9751.503	-39.259	1541.277	-186.112	34637.677	-92.719	8596.720
-140.625	19775.391	-7.640	58.368	-167.097	27921.407	-78.008	6085.217
-178.369	31815.500	-62.981	3966.606	-188.061	35366.940	-87.793	7707.628
-160.072	25623.045	-60.906	3709.529	-203.297	41329.670	-134.929	18205.835
-107.818	11624.721	-66.204	4382.996	-192.424	37026.996	-103.282	10667.172
-105.017	11028.570	-60.078	3609.354	-174.174	30336.582	-86.939	7558.459
-153.844	23667.976	-64.574	4169.789	-189.698	35985.331	-117.614	13833.053
-134.185	18005.614	-64.377	4144.398	-215.241	46328.688	-113.787	12947.481
-119.752	14340.542	-58.784	3455.547	-161.067	25942.578	-106.123	11262.091
-145.542	21182.474	-45.223	2045.093	-183.677	33737.240	-79.933	6389.316
-99.790	9957.984	-52.738	2781.286	-142.711	20366.430	-128.583	16533.588
-105.517	11133.837	-74.188	5503.904	-150.637	22691.506	-55.660	3098.058
-78.655	6186.672	-51.533	2655.660	-88.366	7808.585	-102.592	10525.118
-61.906	3832.402	-17.018	289.609	-72.933	5319.252	-23.637	558.689
	15499.122		2537.283		28228.592		8581.681
	124.495		50.371		168.014		92.637

SET 21

SET 22

CF	CF²	RF	RF²	CF	CF²	RF	RF²
-87.482	7653.170	-16.910	285.941	-125.608	15777.370	-44.312	1963.589
-98.237	9650.469	-93.079	8663.607	-126.338	15961.290	-52.727	2780.137
-120.111	14426.652	-89.223	7960.762	-109.036	11888.849	-39.643	1571.560
-98.200	9643.220	-61.818	3821.515	-95.946	9205.616	-53.078	2817.242
-93.599	8760.754	-31.674	1003.255	-118.364	14010.036	-35.392	1252.601
-140.472	19732.383	-72.678	5282.135	-172.876	29886.111	-85.246	7266.949
-116.517	13576.211	-87.073	7581.638	-152.412	23229.418	-68.889	4745.749
-145.919	21292.355	-85.774	7357.231	-88.609	7851.590	-41.746	1742.703
-66.389	4407.459	-84.535	7146.116	-78.743	6200.413	-21.610	466.996
-156.416	24465.965	-104.843	10992.055	-143.630	20629.577	-92.770	8606.310
-113.029	12775.555	-72.846	5306.481	-130.648	17068.900	-95.824	9182.239
-139.638	19498.771	-92.122	8486.518	-99.945	9989.043	-69.312	4804.153
-130.269	16970.012	-78.133	6104.734	-91.711	8410.963	-12.192	148.633
-134.217	18014.203	-70.429	4960.272	-150.897	22769.905	-69.603	4844.564
-96.934	9396.278	-25.047	627.332	-88.649	7858.716	-16.010	256.333
-127.630	16289.417	-82.850	6864.056	-111.675	12471.306	-60.998	3720.793
-122.720	15060.198	-89.093	7937.474	-59.960	3595.190	-46.583	2169.976
-104.700	10962.090	-49.568	2456.997	-71.367	5093.249	-61.950	3837.840
-62.510	3907.513	-73.598	5416.592	-78.649	6185.728	-75.407	5686.170
-64.932	4216.113	11.100	123.210	-66.374	4405.455	5.775	33.348
	13034.939		5418.896		12624.436		3394.894

114.171

73.613

112.359

58.266

SET 23

SET 24

CF	CF ²	RF	RF ²	CF	CF ²	RF	RF ²
-127.814	16336.419	-44.531	1983.028	-86.547	7490.331	-37.557	1410.506
-90.283	8151.020	-61.301	3757.862	-96.893	9388.195	-33.618	1130.136
-111.673	12470.859	-16.180	261.799	-85.237	7265.295	-77.009	5930.401
-104.729	10968.163	-15.450	238.712	-96.845	9378.973	-37.554	1410.265
-117.169	13728.575	-23.478	551.221	-77.270	5970.668	-14.471	209.395
-129.022	16646.676	-61.516	3784.243	-151.739	23024.724	-124.400	15475.360
-111.341	12396.818	-39.726	1578.179	-110.508	12212.018	-46.804	2190.596
-125.677	15794.708	-48.140	2317.440	-115.099	13247.780	-72.304	5227.854
-139.723	19522.517	-62.254	3875.598	-93.483	8739.127	-37.508	1406.858
-135.993	18494.096	-58.331	3402.447	-106.444	11330.325	-86.045	7403.776
-92.032	8469.871	-17.603	309.852	-68.480	4689.442	-59.705	3564.663
-137.883	19011.722	-53.625	2875.673	-119.242	14218.655	-62.973	3965.599
-133.674	17868.738	-51.644	2667.103	-112.719	12705.573	-58.512	3423.701
-135.397	18332.348	-51.922	2695.863	-108.591	11792.005	-53.560	2868.684
-130.738	17092.425	-53.072	2816.627	-104.520	10924.430	-62.730	3935.040
-136.400	18604.960	-43.464	1889.128	-121.208	14691.379	-73.162	5352.664
-120.653	14557.146	-45.821	2099.546	-121.162	14680.230	-49.802	2480.209
-100.239	10047.857	-42.994	1848.518	-88.954	7912.779	-33.637	1131.428
-77.523	6009.862	-96.377	9288.488	-59.547	3545.869	-47.324	2239.533
-61.655	3801.302	-4.489	20.152	-15.103	228.092	-18.851	355.349
	13915.304		2413.074		10171.795		3555.601
	117.963		49.123		100.855		59.629

SET 25

SET 26

CF	CF ²	RF	RF ²	CF	CF ²	RF	RF ²
-111.332	12394.814	-45.893	2106.204	-134.257	18024.942	-47.828	2287.489
-111.818	12503.265	-61.459	3777.196	-90.536	8196.804	-84.662	7167.654
-128.843	16600.519	-77.025	5932.804	-129.219	16697.550	-34.307	1176.984
-106.623	11368.464	-41.377	1712.081	-23.736	563.379	-5.282	27.904
-119.651	14316.362	-55.715	3104.161	-127.317	16209.618	-22.478	505.265
-115.846	13420.296	-39.689	1575.233	-158.211	25030.721	-99.983	9996.580
-95.423	9105.530	-74.002	5476.296	-135.098	18251.470	-82.711	6841.126
-76.245	5813.361	-11.099	123.181	-157.297	24742.346	-81.153	6585.842
-94.194	8872.472	-59.356	3523.087	-149.526	22358.025	-69.654	4851.610
-128.082	16404.999	-77.153	5952.555	-136.862	18731.207	-57.243	3276.704
-113.840	12959.546	-74.542	5556.450	-102.883	10584.912	-52.146	2719.216

-135.362	18322.871	-155.696	24241.244	-155.949	24320.091	-116.668	13611.422
-71.358	5091.993	-53.626	2875.759	-65.992	4354.944	-29.470	868.451
-143.177	20499.653	-75.704	5731.020	-156.984	24643.976	-70.637	4989.572
-131.290	17237.064	-62.397	3893.361	-135.649	18400.651	-59.290	3515.328
-137.072	18788.733	-54.699	2992.013	-137.441	18890.028	-71.205	5070.124
-106.801	11406.454	-66.769	4458.033	-72.894	5313.491	-64.494	4159.412
-86.947	7559.850	-16.550	273.916	-105.120	11050.214	-42.844	1835.608
-82.609	6824.296	-43.516	1893.642	-78.791	6208.037	-66.660	4443.556
-51.477	2649.851	-8.262	68.257	-73.630	5421.436	-5.954	35.455
	12107.020		4263.325		14899.692		4198.265
	110.032		65.294		122.064		64.794

SET 27

SET 28

CF	CF²	RF	RF²	CF	CF²	RF	RF²
-194.241	37729.566	-58.436	3414.766	-73.872	5457.043	-29.802	888.147
-154.432	23849.243	-69.488	4828.624	-77.181	5956.891	-65.126	4241.448
-154.229	23786.584	-113.269	12829.866	-25.482	649.322	-1.539	2.367
-141.624	20057.357	-40.260	1620.835	-76.054	5784.180	-34.625	1198.918
-175.596	30833.955	-27.396	750.541	-95.400	9101.160	-37.046	1372.414
-184.926	34197.625	-72.612	5272.517	-131.279	17234.176	-65.549	4296.619
-174.967	30613.451	-158.738	25197.753	-106.980	11444.720	-61.784	3817.238
-207.093	42887.511	-72.865	5309.308	-75.610	5716.812	-32.047	1026.985
-178.663	31920.468	-47.684	2273.773	-111.614	12457.685	-63.549	4038.425
-205.893	42391.927	-93.374	8718.648	-129.335	16727.542	-67.728	4587.136
-245.507	60273.687	-128.589	16535.131	-106.690	11382.756	-60.515	3662.102
-181.687	33010.166	-65.745	4322.339	-119.418	14260.659	-62.262	3876.606
-429.208	184219.507	-41.376	1711.957	-107.799	11620.624	-54.254	2943.442
-168.723	28467.451	-112.561	12669.979	-117.257	13749.204	-69.098	4774.478
-202.241	40901.422	-86.528	7487.026	-119.272	14225.810	-51.461	2648.265
-142.166	20211.172	-63.120	3984.160	-106.572	11357.591	-48.287	2331.625
-142.374	20270.356	-142.789	20388.699	-115.578	13358.274	-71.864	5164.478
-147.820	21850.752	-59.469	3536.514	-75.490	5698.740	-45.437	2064.494
-102.358	10477.160	-13.827	191.186	-65.475	4286.963	-48.658	2367.620
-1.823	3.323	-0.283	0.080	-45.310	2052.960	-1.307	1.707
	36897.634		7052.185		9626.156		2765.226
	192.088		83.977		98.113		52.585

SET 29

SET 30

CF	CF ²	RF	RF ²	CF	CF ²	RF	RF ²
-176.644	31203.103	-60.021	3602.520	-126.746	16064.549	-48.638	2365.616
-165.376	27349.221	-85.953	7387.867	-120.887	14613.667	-45.398	2060.987
-135.668	18405.806	-42.927	1842.684	-128.701	16563.947	-27.446	753.255
-156.622	24530.451	-30.424	925.632	-114.536	13118.495	-35.097	1231.813
-197.572	39034.695	-109.608	12013.914	-129.301	16718.749	-100.228	10045.652
-153.499	23561.943	-102.645	10535.996	-146.755	21537.030	-80.691	6510.989
-182.645	33359.196	-90.799	8244.368	-109.228	11930.756	-66.840	4467.559
-182.509	33309.535	-90.120	8121.668	-126.746	16064.549	-57.212	3273.167
-201.399	40561.557	-112.115	12569.773	-68.630	4710.049	-76.242	5812.888
-214.385	45960.928	-153.262	23489.241	-151.511	22955.583	-100.499	10100.049
-73.865	5456.068	-6.988	48.834	-171.277	29335.811	-125.761	15815.829
-144.142	20776.916	-76.330	5826.193	-152.935	23389.114	-105.807	11195.121
-123.294	15201.410	-35.325	1247.884	-148.337	22003.866	-82.519	6809.369
-164.046	26911.090	-61.641	3799.601	-110.940	12307.684	-53.845	2899.284
-160.518	25766.028	-76.094	5790.297	-136.473	18624.880	-89.210	7958.335
-170.586	29099.583	-104.418	10903.119	-118.403	14019.270	-97.028	9414.433
-170.903	29207.835	-63.253	4000.967	-39.843	1587.473	-3.233	10.453
-157.574	24829.565	-173.173	29988.888	-100.002	10000.400	-91.397	8353.430
-91.143	8306.955	-95.703	9159.141	-91.068	8293.399	-34.209	1170.276
-87.687	7689.063	-17.266	298.111	-69.551	4837.356	-0.926	0.857
	25526.048		7989.835		14933.831		5512.468
	159.769		89.386		122.204		74.246

SET 31				SET 32			
CF	CF ²	RF	RF ²	CF	CF ²	RF	RF ²
-117.982	13919.752	-48.086	2312.302	-65.753	4323.483	-25.212	635.635
-120.243	14458.379	-56.616	3205.417	-50.692	2569.709	-72.533	5261.007
-119.858	14365.940	-80.658	6505.681	-83.468	6966.940	-121.553	14775.132
-116.541	13581.805	-27.044	731.351	-72.367	5236.983	-14.648	214.561
-118.539	14051.495	-67.065	4497.701	-77.592	6020.581	-25.437	647.031
-137.326	18858.430	-59.165	3500.497	-82.031	6729.036	-50.686	2569.071
-131.233	17222.100	-45.944	2110.879	-87.575	7669.416	-51.049	2605.960
-122.044	14894.738	-39.349	1548.336	-89.377	7988.195	-42.312	1790.271
-138.734	19247.123	-59.579	3549.669	-80.768	6523.389	-77.716	6039.777
-130.816	17112.826	-70.232	4932.590	-96.018	9219.495	-69.535	4835.102
-125.747	15812.308	-69.205	4789.304	-84.207	7090.768	-50.514	2551.644
-119.480	14275.470	-49.992	2499.240	-94.979	9020.953	-52.401	2745.886
-135.059	18240.933	-78.317	6133.505	-39.062	1525.809	-34.620	1198.524
-113.750	12939.063	-77.014	5931.202	-95.685	9155.619	-52.278	2732.989

-150.617	22685.481	-65.253	4257.993	-38.323	1468.675	-29.803	888.189
-77.427	5994.971	-13.777	189.817	-100.767	10153.988	-67.804	4597.355
-129.567	16787.607	-82.884	6869.791	-83.160	6915.635	-36.364	1322.355
-89.756	8056.175	-58.167	3383.435	-57.873	3349.296	-42.877	1838.471
-71.694	5140.001	-63.562	4040.077	-52.684	2775.625	-39.242	1539.911
-59.460	3535.515	-20.795	432.436	-41.671	1736.447	-1.194	1.425
	14059.006		3571.061		5822.002		2939.515
	118.571		59.758		76.302		54.217

REFERENCES

- [1] Aleksandra. (2023, May 4). Tungsten Carbide - Properties and Applications of Tungsten Carbide: Part 1. *SOLLEX*.
- [2] Altintas, Y. (2000). *Manufacturing Automation*. Cambridge University Press.
- [3] Ambadekar, K. P., & Choudhari, S. C. (2020). Measurement of Tungsten Carbide Tool Wear by Tribological Investigations. *Journal of Bio- and Tribo-Corrosion*.
- [4] Armero, F., & Love, E. (2001). ALE finite element methods for finite strain plasticity and fluid problems. *Proceedings of the 2nd European Conference on Computational Mechanics*. Cracow, Poland.
- [5] Armero, F., & Love, E. (2003). *International Journal for Numerical Methods in Engineering*, 471-508.
- [6] Arrazola, J. P., Garay, A., Iriarte, M. L., Armendia, M., Marya, S., & Le Maitre, F. (2009). Machinability of titanium alloys (Ti6Al4V and Ti555.3). *Journal of Materials Processing Technology*, 2223-2230.
- [7] Auchet, S., Chevrier, P., Lacour, M., & Lipinski, P. (2004). A new method of cutting force measurement based on command voltages of active electro-magnetic bearings. *International Journal for Machining Tools and Manufacture*, 1441-1449.
- [8] Barile, C., Casavola, C., Pappalettera, G., & Pappalettera, C. (2011). Experimental and numerical characterization of sinterized materials with speckle interferometry and optimization methods. *10th IMEKO TC15 Youth Symposium on Experimental Solid Mechanics*, (pp. 35-36). Chemnitz.
- [9] Barile, C., Casavola, C., Pappalettera, G., & Pappalettera, C. (n.d.). *Advanced Approaches for Mechanical Characterization On Innovative Materials*.
- [10] Benson, D. (1989). An efficient, accurate, simple ALE method for nonlinear finite element programs. *Computer Methods in Applied Mechanics and Engineering*, 305-350.
- [11] Bermingham, M. J., Palanisamy, S., & Dargush, M. S. (2012). Understanding the tool wear mechanism during thermally assisted machining Ti-6Al-4V. *International Journal of Machine Tools & Manufacture*, 76-87.
- [12] Bolzoni, L., Ruiz-Navas, E., & Gordo, E. (2017). Quantifying the properties of low-cost powder metallurgy titanium alloys. *Material Science and Engineering*, 47-53.
- [13] Boothroyd, G. (1961). Photographic technique for the determination of metal cutting temperatures. *Journal of Applied Physics*, 238-242.

- [14] Chen, G., Ren, C., Yu, W., Yang, X., & Zhang, L. (2012). , Application of genetic algorithms for optimizing the Johnson–Cook constitutive model. *Proceedings of the Institution of Mechanical Engineers, Part B: Journal of Engineering Manufacture*, 1287-1297.
- [15] Childs, T. (2000). *Metal Machining: Theory and Applications*. Butterworth-Heinemann: Oxford.
- [16] Clement, N., Lenain, A., & Jacques, P. J. (2007). Mechanical property optimization via microstructural control of new metastable beta titanium alloys, processing and characterizing titanium alloys overview. *Materials*, 50-53.
- [17] Connolly, R., & Rubenstein, C. (1968). The mechanics of continuous chip formation in orthogonal cutting. *International Journal of Machine Tools and Manufacture*, 159-187.
- [18] Dillon, W. O., De Angelis, J. R., Lu, Y. W., Gunasekara, S. J., & Deno, A. J. (1990). The effects of temperature on machining of metals. *Material Shaping Technologies*, 23.
- [19] Ding, Y., & Hong, S. (1998). Improvement of chip breaking in machining low carbon steel by cryogenically pre-cooling the workpiece. *Manufacturing Science and Engineering*, 76-83.
- [20] Donea, J., Stella, F. P., & Giuliani, S. (1977). Lagrangian and Eulerian finite element techniques for transient fluid-structure interaction problems. *Transactions of the 4th International Conference on Structural Mechanics in Reactor Technology* (pp. 1-12). San Francisco: CA.
- [21] Dorogoy, A., & Rittel, D. (2009). Determination of the Johnson–Cook material parameters using the SCS specimen. *Exp. Mech.*, 881-885.
- [22] Ducobu, F., Arrazola, J. P., Lorphevre, R., Zarate, O. G., Madariaga, A., & Filippi, E. (2017). The CEL method as an alternative to the current modelling approaches for Ti6Al4V orthogonal cutting simulation. *16th CIRP Conference on Modelling of Machining Operations*, (pp. 245-250).
- [23] Ducobu, F., Arrazola, P.-J., Riviere, L. E., & Filippi, E. (2015). Comparison of several behaviour laws intended to produce a realistic Ti6Al4V chip by finite elements modelling. *Engineering*, 651-653 & 1197-1203.
- [24] Ducobu, F., Lorphevre, R. E., & Filippi, E. (2017). On the importance of the choice of the parameters of the Johnson-Cook constitutive model and their influence on the results of a Ti6Al4V orthogonal cutting model. *International Journal of Mechanical Sciences*, 143-155.
- [25] Ducobu, F., Lorphevre, R. E., Fernandez, G. M., Soberanis, A. S., Arrazola, J. P., & Ghadbeigi, H. (2019). Coupled Eulerian-Lagrangian (CEL) simulation for modelling of chip formation in AA2024-T3. *17th CIRP Conference on Modelling of Machining Operations*, (pp. 142-147).
- [26] Ducobu, F., Riviere-Lorphevre, E., & Filippi, E. (2015). Experimental contribution to the study of the Ti6Al4V chip formation in orthogonal cutting on a milling machine. *Int J Mater Form*, 8, 455–468. doi:DOI 10.1007/s12289-014-1189-4

- [27] Fang, N., & Wu, Q. (2009). A comparative study of the cutting forces in high speed machining of Ti-6Al-4V and Inconel 718 with a round cutting edge tool. *Journal of Materials Processing Technology*, 4385-4389.
- [28] Grzesik, W. (1999). Experimental investigation of the cutting temperature when turning with coating indexable inserts. *International Journal of Machine tool and Manufacture*, 355-369.
- [29] Guo, B. Y., & Yen, W. D. (2004). A FEM study on mechanisms of discontinuous chip formation in hard machining. *Journal of Materials Processing Technology*, 1350-1356.
- [30] Hong, Y. S., Markus, I., & Jeong, C. W. (2001). New cooling approach and tool life improvement in cryogenic machining of titanium alloy Ti-6Al-4V. *International Journal of Machine Tools & Manufacture*, 2245-2260.
- [31] Hua, J., & Shivpuri, R. (2004). Prediction of chip morphology and segmentation during the machining of titanium alloys. *Journal of Materials Processing Technology*, 124-133.
- [32] Johnson, G., & Cook, W. (1983). A constitutive model and data for metals subjected to large strains, high strain rates and high temperatures. *Proceedings of the seventh international symposium on ballistics* (pp. 541-547). The Netherlands: The Hague.
- [33] Kandrak, L., Mankova, I., Vrabel, M., & Beno, J. (2014). Finite Element Simulation of Cutting Forces in Orthogonal Machining of Titanium Alloy Ti-6Al-4V. *Applied Mechanics and Materials*, 192-199.
- [34] Komanduri, R., & von Turkovich, B. (1981). New Observations on the Mechanism of Chip Formation when Machining Titanium Alloys. *Wear*(69), 179-188.
- [35] Kountanya, R., Zkeri, A. I., & Altan, T. (2009). Effect of tool edge geometry and cutting conditions on experimental and simulated chip morphology in orthogonal hard turning of 100Cr6 steel. *Journal of Materials Processing Technology*, 5068-5075.
- [36] Krishnaraj, V., Samsudeensadham, S. S., & Kuppan, P. (2014). A study on high speed end milling of titanium alloy. *12th Global Congress on Manufacturing and Management* (pp. 251-257). GCMM.
- [37] Li, Z., Qu, H., Chen, F., Wang, Y., Tan, Z., Kopec, M., . . . Zheng, K. (2019, January 10). Deformation Behaviour and Microstructural Evolution during Hot Stamping of TA15 Sheets: Experimentation and Modelling.
- [38] Liang, X., & Liu, Z. (2018). Tool wear behaviors and corresponding machined surface topography during high-speed machining of Ti-6Al-4V with fine grain tools. *Tribology International*, 321-332.
- [39] Lin, C. Z., & Lin, Y. Y. (1999). A study of an oblique cutting model. *Journal of Materials Processing Technology*, 119-130.

- [40] Lin, J., & Yang, J. (1999). GA-based multiple objective optimisation for determining viscoplastic constitutive equations for superplastic alloys. *International Journal of Plasticity* 15, 1181-1196.
- [41] Liu, W. K. (1981). Finite element procedures for fluid-structure interactions and applications to liquid storage tanks. *Nuclear Engineering and Design*, 221-238.
- [42] Lopez, A. I. (2018). Subsurface deformation micromechanisms induced during machining of titanium alloys at low temperatures, and a novel testing methodology to examine their machining behaviour. Sheffield.
- [43] Movahhedy, M., Gadala, S. M., & Altintas, Y. (2000). Simulation of the orthogonal metal cutting process using an arbitrary Lagrangian-Eulerian finite-element method. *Journal of Materials Processing Technology*, 267-275.
- [44] Nouari, M., & Ginting, A. (2006). Wear characteristics and performance of multi-layer CVD-coated alloyed carbide tool in dry end milling of titanium alloy. *Surface Coating Technologies*, 18-19.
- [45] Nouari, M., & Makich, H. (2013). Experimental investigation on the effect of the material microstructure on tool wear when machining hard titanium alloys: Ti-6Al-4V and Ti-555. *International Journal of Refractory Metals and Hard Materials*, 259-269.
- [46] Obikawa, T., Sasahara, H., Shirakashi, T., & Usui, E. (1997). Application of computational machining method to discontinuous chip formation. *ASME Journal of Manufacturing Science and Engineering*, 667-674.
- [47] Pederson, R. (2002). *Microstructure and Phase Transformation of Ti-6Al-4V*. Department of Applied Physics and Mechanical Engineering - Lulea University of Technology.
- [48] Pednecker, V., Madhavan, V., & Adibi-Sedeh, H. A. (2004). Investigation of the transition from plane strain to plane stress in orthogonal metal cutting. *ASME 2004 International Mechanical Engineering Congress and Exposition*, (pp. 513-528).
- [49] Revuru, S. R., Pasam, K. V., & Posinasetti, R. N. (2020, June 1-5). Performance of coated cutting tools in machining: A review. *The International Conference on Emerging Trends in Engineering and Technology*.
- [50] Rott, O., Homberg, D., & C, M. (2006). A comparison of analytical cutting force models.
- [51] Sasahara, S., Obikawa, T., & Shirakashi, T. (2004). Prediction model of surface residual stress within a machined surface by combining two orthogonal plane models. *International Journal of Machine Tools and Manufacture*, 815-822.
- [52] Schulz, H. (2004). Why High Speed Cutting (HSC). *Proceedings of the International Conference on High Speed Machining* (pp. 1-20). Nanjing, China: PR.

- [53] Shaw, M. C., & Vyas, A. (1998, May 19-22). Hard turning of steel. *Proceedings of the 1998 XXVI NAMRC Conference*, pp. 1-5.
- [54] Shet, C., & Deng, X. (2000). Finite element analysis of the orthogonal metal cutting process. *Journal of Materials Processing Technology*, 95-109.
- [55] Sisodiya, S. M., & Bajpai, V. (2013). An Insight: Machining of Titanium Alloys & Associated Tool Wear. *IOP Conference Series: Materials Science and Engineering*.
- [56] Sun, S., Brandt, M., & John, P. M. (2013). Evolution of tool wear and its effect on cutting forces during dry machining of Ti-6Al-4V alloy. *Proceedings of the Institution of Mechanical Engineers, Part B: Journal of Engineering Manufacture*, 1-12.
- [57] Tyan, T., & Yang, H. W. (1992). Analysis of Orthogonal Metal Cutting Processes. *International Journal for Numerical Methods in Engineering*, Vol. 34, 365-389.
- [58] Umbrello, D. (2008). Finite element simulation of conventional and high speed machining of Ti6Al4V alloy. *Journal Of Materials Processing Technology*, 79-87.
- [59] Usui, E., Shirakashi, T., & Kitagawa, T. (1978). Analytical prediction of three dimensional cutting process—Part 3: Cutting temperature and crater wear of carbide tool. *Journal of Manufacturing Science and Engineering*.
- [60] Venugopal, K. A., Paul, S., & Chattopadhyay, A. B. (2007). Growth of tool wear in turning of Ti-6Al-4V alloy under cryogenic cooling. *Wear*, 294-301.
- [61] Zhao, H., Barber, G., & Zou, Q. (2002). A study of flank wear in orthogonal cutting with internal cooling. *Wear*, 957-962.
- [62] Zhao, Z., & Hong, Y. S. (1992). Cryogenic properties of some cutting tool materials. *Material Engineering and Performance*, 705-714.